High resolution neutron transmission imaging with single pixel spectroscopic resolution

A.S. Tremsin[1], T. Shinohara[2], A.S. Losko[3], S.C. Vogel[3], W. Kockelman[4]

[1]University of California at Berkeley, Berkeley, CA 94720, USA
[2]Japan Atomic Energy Agency, Naka-gun Ibaraki 319-1195, Japan
[3]Los Alamos National Laboratory, Los Alamos, NM 87545, USA
[4]STFC-Rutherford Appleton Laboratory, Didcot, OX11 0QX, UK

The work done in collaboration

University of California at Berkeley, CA, USA
A.S. Tremsin, J. B. McPhate, J. V. Vallerga, O. H. W. Siegmund

Nova Scientific, Inc, Sturbridge, USA (manufacturer of neutron sensitive MCPs)
W. B. Feller, P. White, B. White

Rutherford Appleton Laboratory, ISIS Facility, UK
W. Kockelmann, J. Kelleher, S. Kabra, D.E. Pooley, G. Burca, T. Minniti, E. Schooneveld, N. Rhodes

J-PARC Center, JAEA, Nagoya University, Japan
Y. Kiyanagi, T. Shinohara. T. Kai, K. Oikawa

LANSCE, Los Alamos National Laboratory
S. Vogel, A. Losko, M. Mocko, M.A.M. Bourke, R. Nelson

Paul Scherrer Institute, Switzerland
E. Lehmann, A. Kaestner, T. Panzner, P. Trtik, M. Mangano

Istituto dei Sistemi Complessi, Sesto Fiorentino (FI), Italy
F. Grazzi

ANSTO
A. Sokolova, A. Paradowska, V. Luzin, F. Salvemini

CONICET and Instituto Balseiro, Centro Atomico Bariloche, Argentina
J. Santisteban

Spallation Neutron Source, Oak Ridge National Laboratory, USA
H. Z. Bilheux, L.J. Santodonato

Technische Universität München, Forschungs-Neutronenquelle FRM-II, Germany
B. Schillinger, M. Lerche

Department of Geology and Environmental Earth Science, Miami University
John Rakovan

Welding Science, Cranfield University
Supriyo Ganguly

University of Newcastle, Latrobe University, Australia
C. Wensrich, E. Kisi. H. Kirkwood

Lawrence Berkeley Laboratory
D. Perrodin, G.A. Bizarri, E.D. Bourret

European Spallation Source Scandinavia
M. Strobl, R. Woracek

Technical University of Denmark
S. Schmidt

General Electric Global Research
Yan Gao

…and many others!
apologies for missed names

Outline

- From single pixel neutron spectroscopy to spectroscopic imaging

- Energy-resolved imaging applications
  - *Studies of microstructure*
  - *Elemental composition*
  - *Studies of nuclear fuels*
  - *Imaging of gas pressure/distribution*
  - *Remote temperature measurement*
  - *Characterization of crystal growth*

- One of the enabling technologies
  - *MCP/Timepix detectors for neutron imaging*

Neutron cross sections vs. energy

Thermal range
1-5 Å (~4-100meV)

Bragg edges

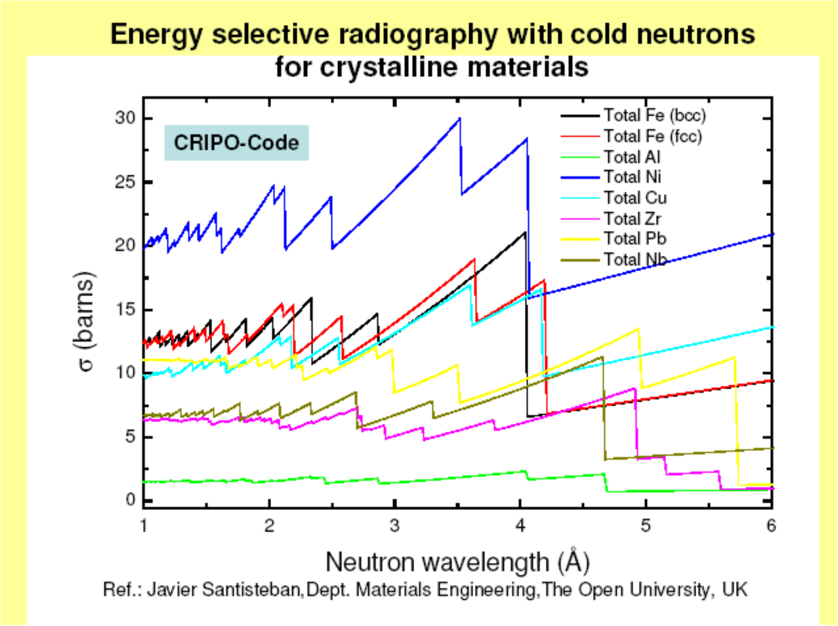

Crystallographic parameters extracted
Phase
Texture
Lattice parameter

Epithermal range
1eV-10 keV (~2-300 mÅ)

Resonance attenuation

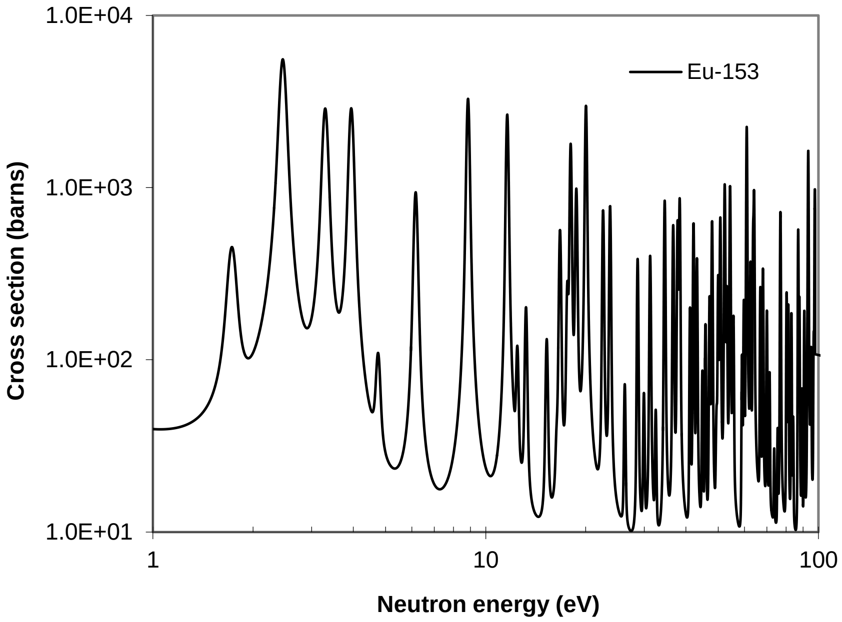

Elemental/isotopic composition
Temperature map

Measured transmission spectra

Polycrystalline materials | **Single crystal materials**

Bragg edges

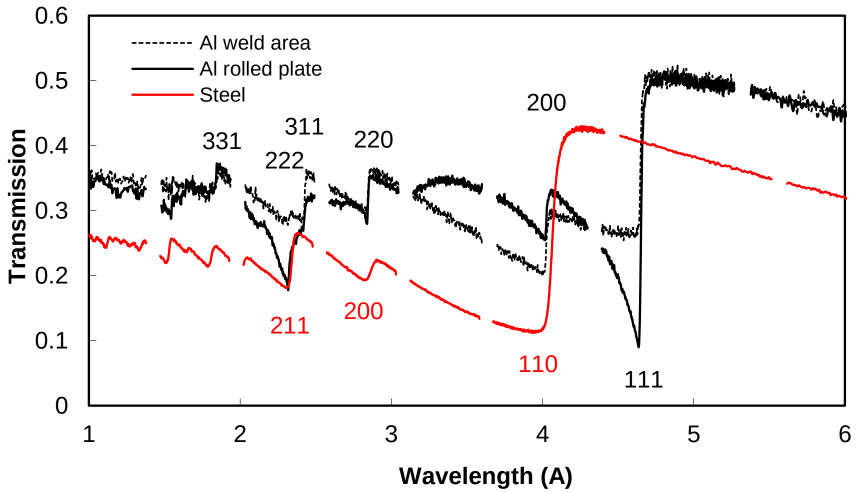

Bragg dips

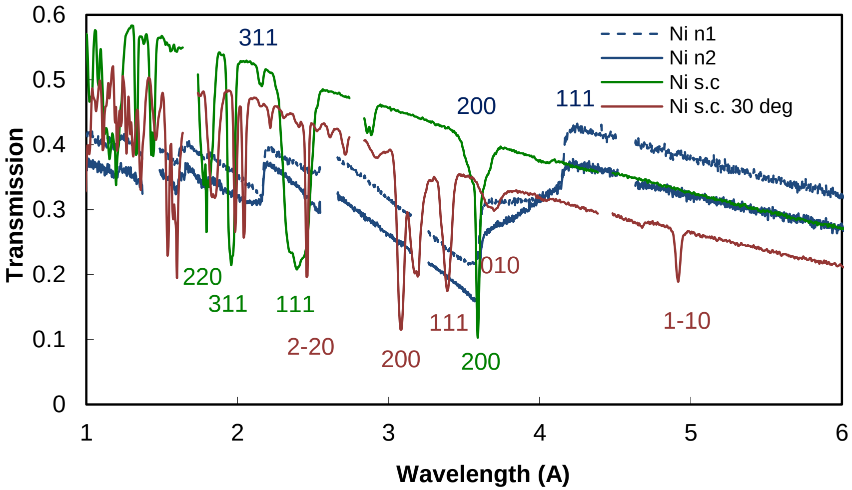

Uniformity of crystallographic parameters can be imaged (integrated through the sample thickness)

Phase
Texture
Lattice parameter

It all started with single pixel transmission spectroscopy

Remote temperature measurement

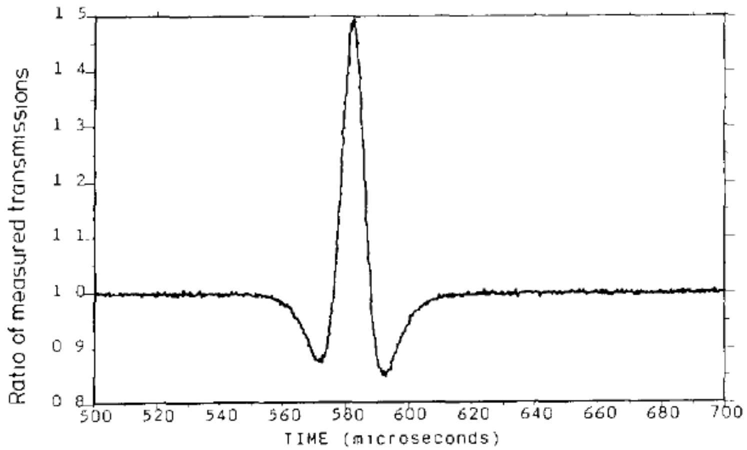

Fig. 1. Measured ratio of transmissions for a 0.004 cm thick rhenium foil near the 2156 meV resonance ($T = 592.2°$ C)/($T = 146.4°$ C)

J. Mayers, et al., Temperature measurement by neutron resonance radiography, NIM A275 (1989) 453-459

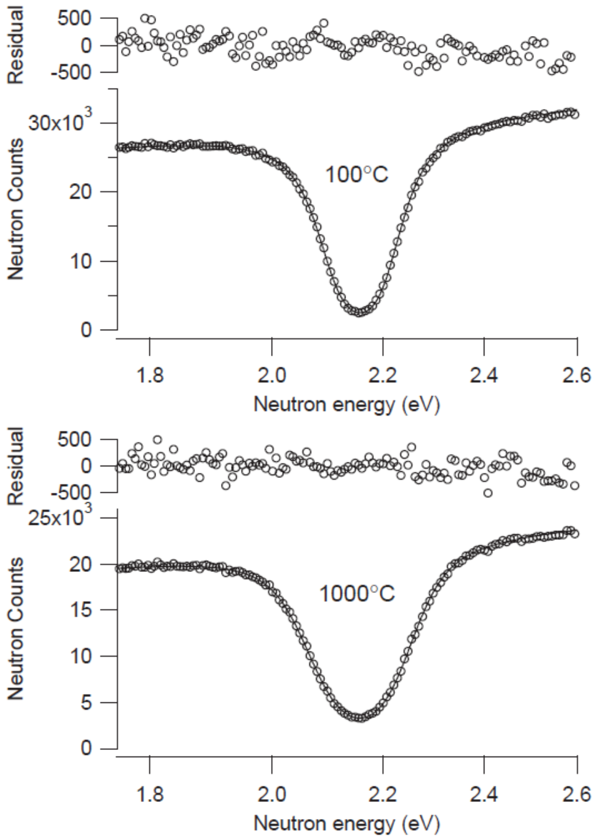

H.J. Stone, et al., NIM A 547 (2005) 601

Remote temperature measurement

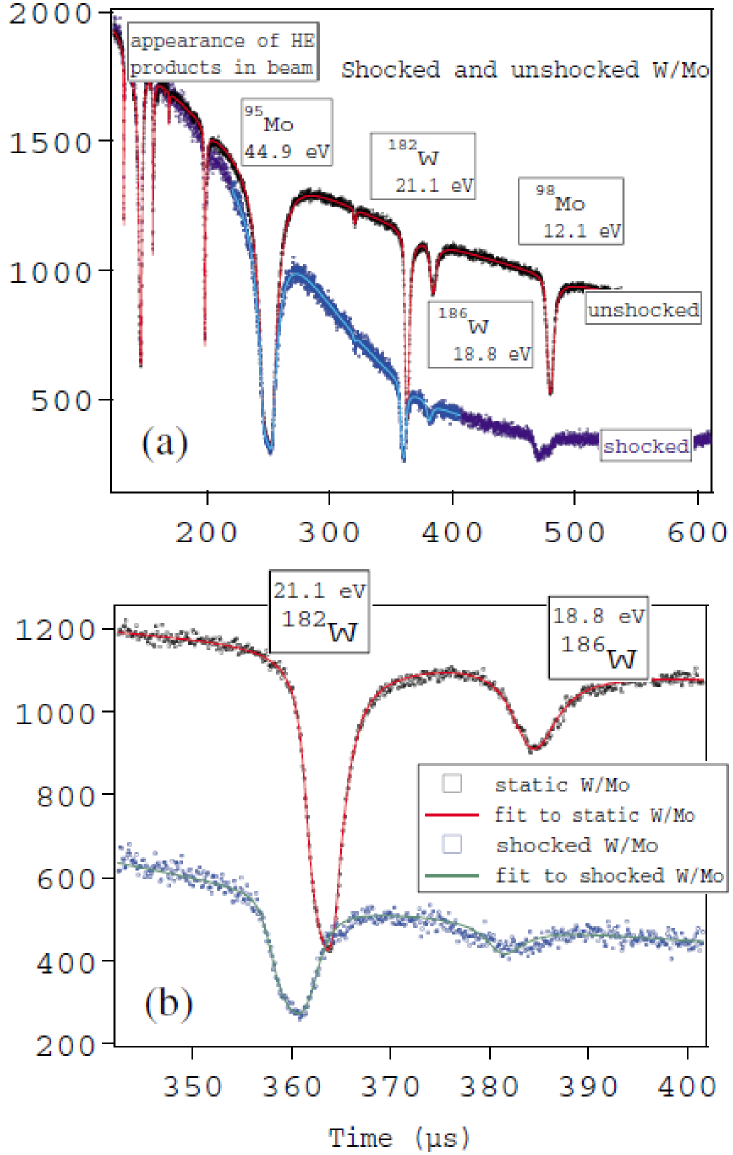

Single pulse spectrum!!!!

We report a direct measurement of temperature in a shocked metal using Doppler broadening of neutron resonances. The 21.1-eV resonance in ^{182}W was used to measure the temperature in molybdenum shocked to 63 GPa. An explosively launched aluminum flyer produced a planar shock in a molybdenum target that contained a 1-mm thick layer doped with 1:7 at:%^{182}W. A single neutron pulse, containing resonant neutrons of less than 1 s duration, probed the shocked material. Fits to the neutron time-of-flight data were used to determine the temperature of the shocked molybdenum.

V.W. Yuan, et al., Shock Temperature Measurement Using Neutron Resonance Spectroscopy, PRL 94, 125504 (2005)

Resonance imaging (as early as 1980)

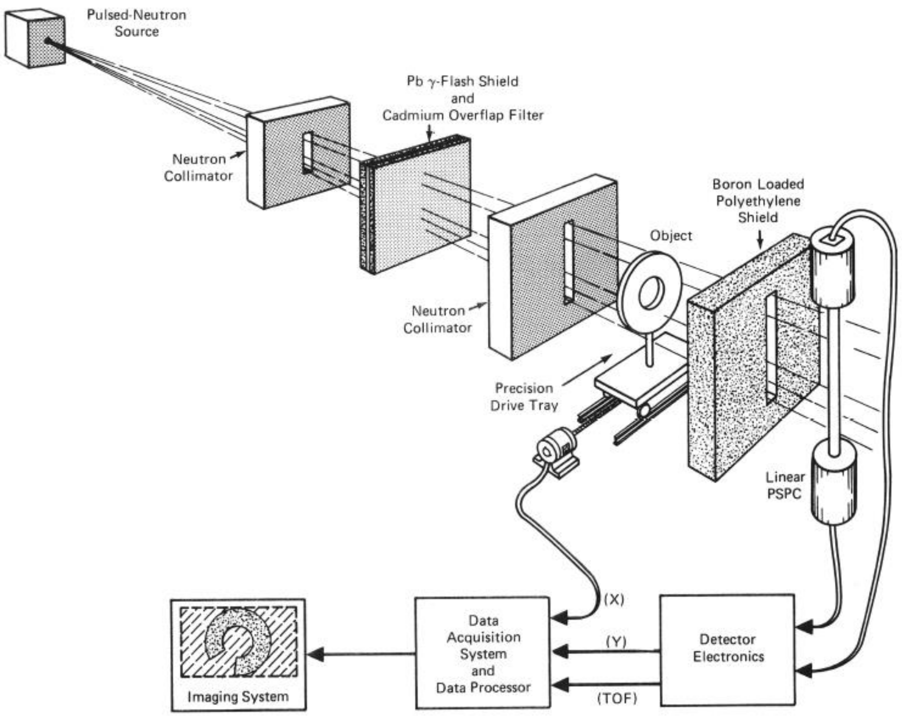

Fig. 1. Illustration of experimental setup for resonance neutron radiography.

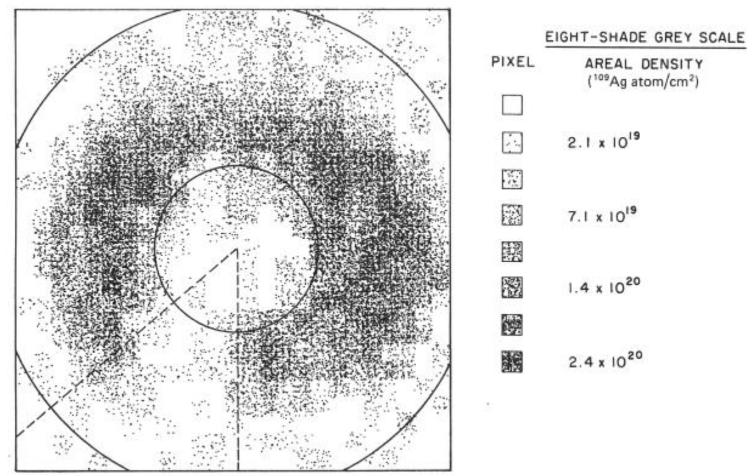

Fig. 4. Eight-shade grey-scale representation of silver distribution in silver-brazed object.

NONDESTRUCTIVE EXAMINATION OF A DEFECTIVE SILVER BRAZE USING RESONANCE-NEUTRON RADIOGRAPHY

J. W. BEHRENS, R. A. SCHRACK, and C. D. BOWMAN
National Bureau of Standards, Washington, D.C. 20234

NUCLEAR TECHNOLOGY VOL. 51 NOV. 1980

Extension to multi-pixel detectors

Energy-resolved imaging

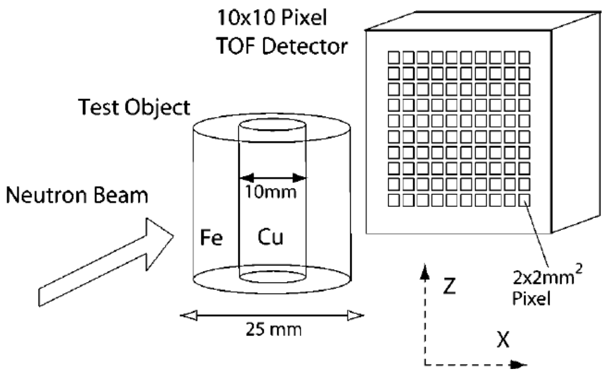

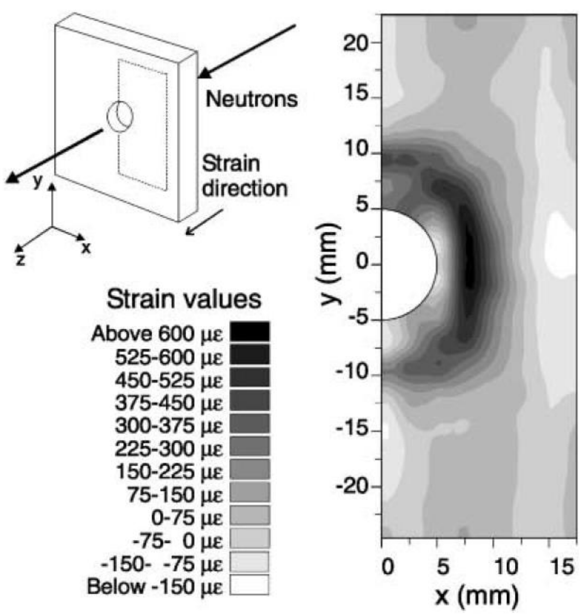

J.R. Santisteban, et al., Appl. Phys. A 74 [Suppl.], S1433–S1436 (2002) /

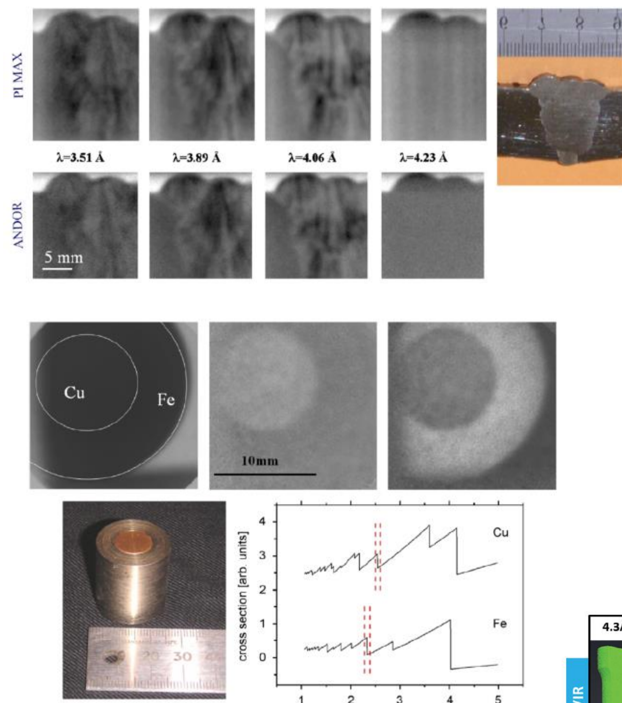

W. Kocklemann, et al., NIM A 578 (2007) 421–434

R. Woracek, et al., Adv. Mater. **2014**, *26*, 4069–4073

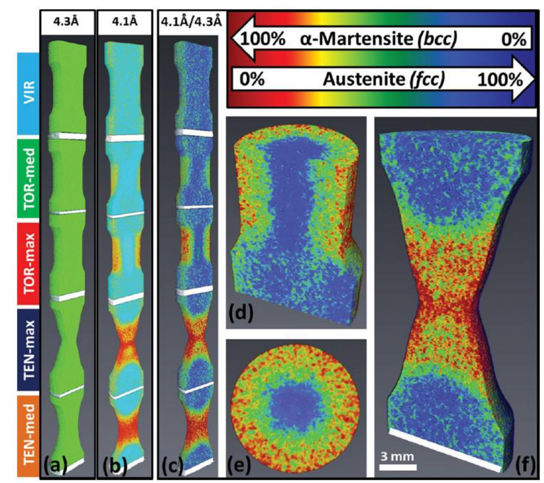

Cultural heritage studies

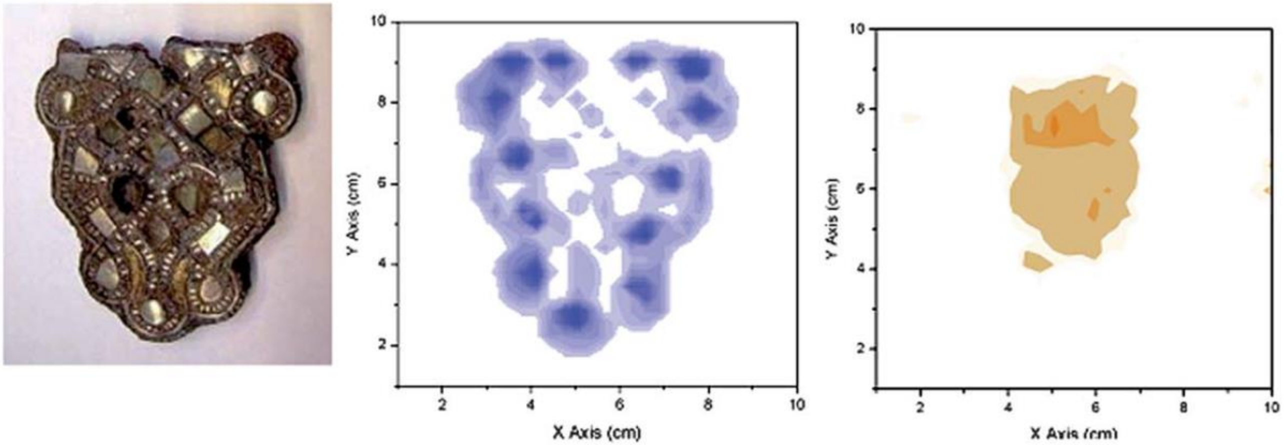

E. P. Cippo, et al., J. Anal. At. Spectrom., 2011, 26, 992

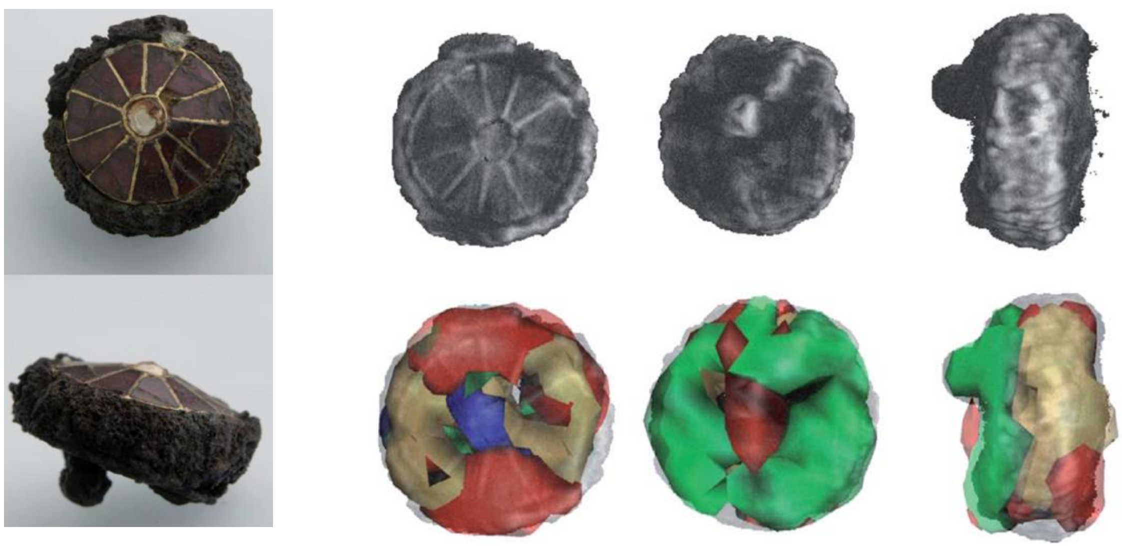

First 3D tomography with resonance imaging!

Giulia Festa, et al., Neutron resonance transmission imaging for 3D elemental mapping at the ISIS spallation neutron Source, J. Anal. At. Spectrom., 2015,30, 745

Energy-resolved imaging with neutrons

Pulsed Neutron Source
20 - 60 Hz
100-600 ns pulses

Propagating neutron pulse

Neutron counting
2D detector

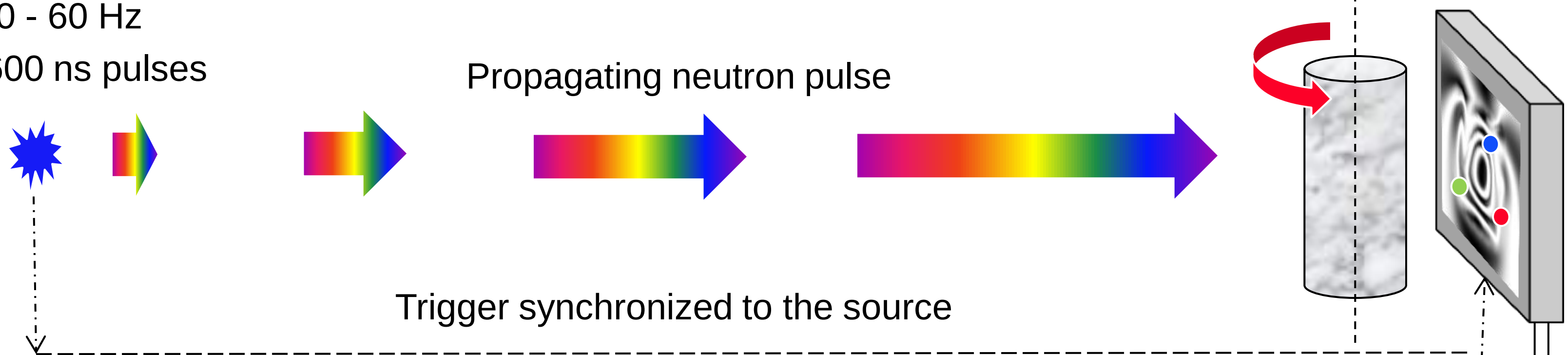

Trigger synchronized to the source

Sample

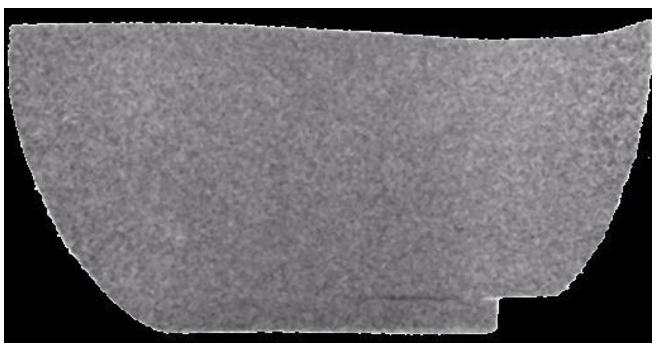

All energies are imaged at the same time

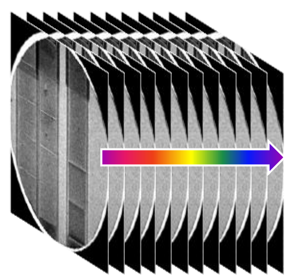

X,Y,T for every detected neutron

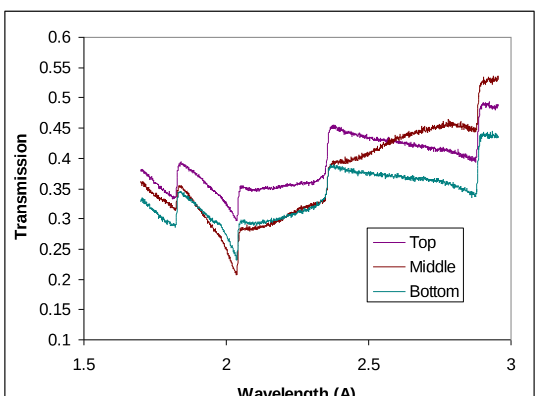

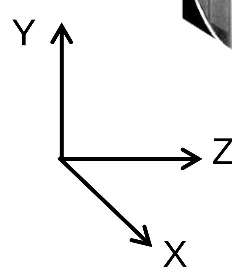

~250,000 spectra are measured simultaneously!

Detector configuration

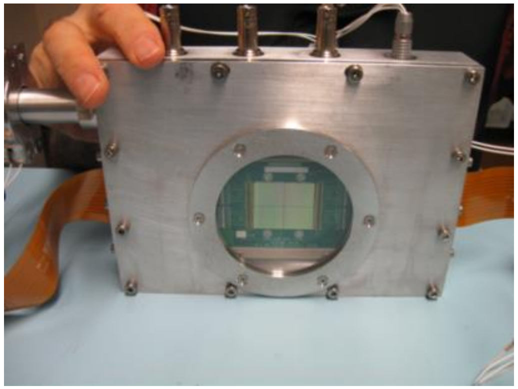

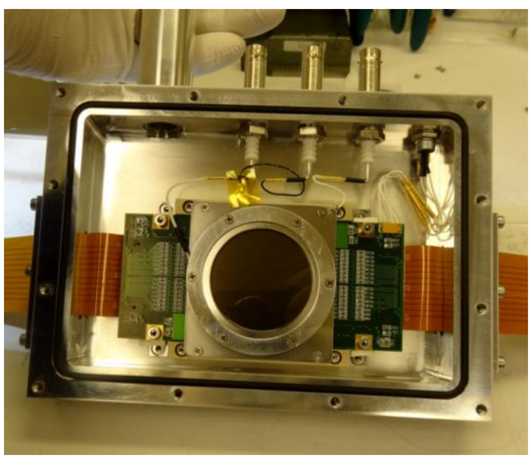

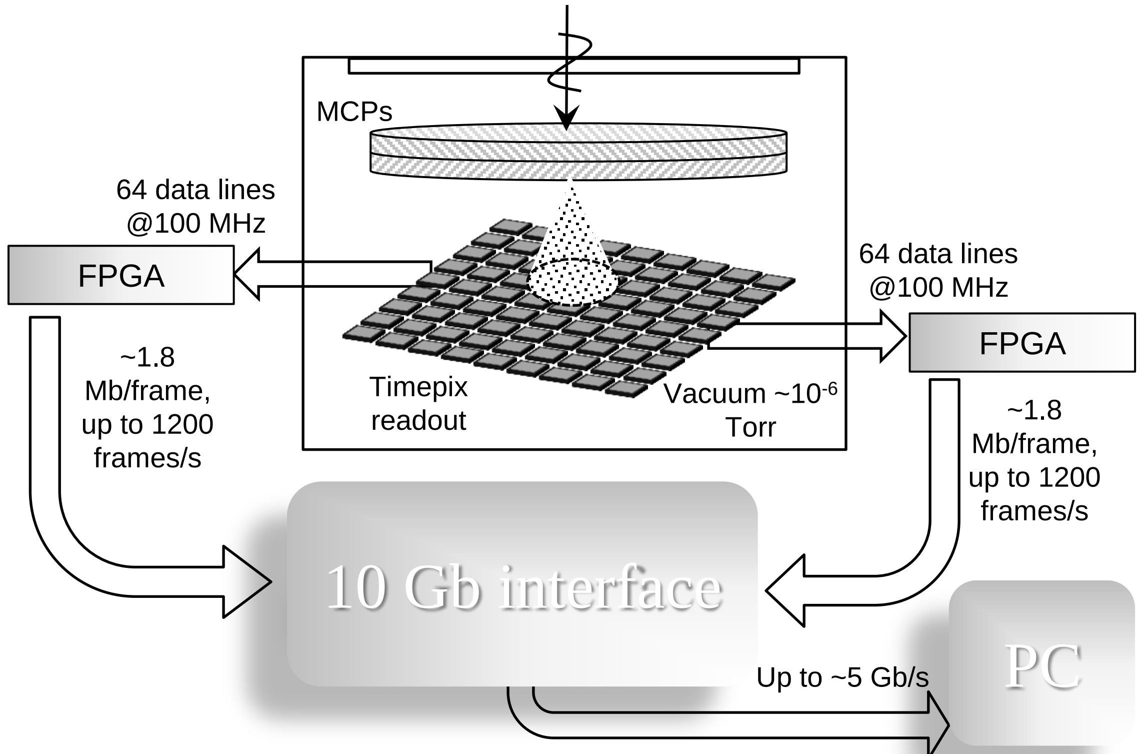

Enabling technology

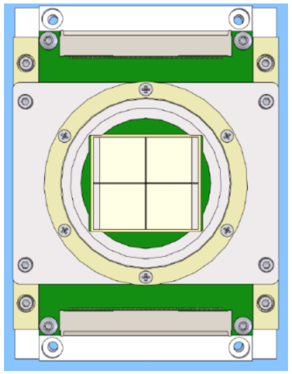

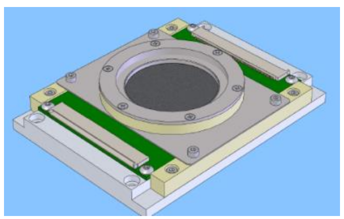

- **Bright pulsed neutron beams**

- **New neutron counting detectors with high timing and spatial resolution @ high count rates**

~250000 spectra are measured at the same time, each within 55 um pixel!

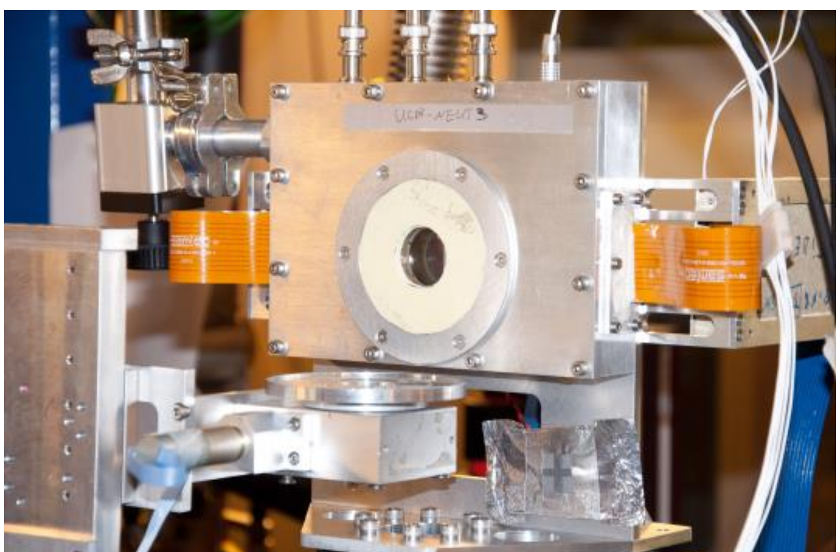

- Active area with 2x2 Timepix chips (28x28 mm^2)
- Fast parallel readout (x32) allowing ~1200 frames per second and ~300 μs dead time
- Fast event counting capability with XY and Time of arrival
- Wide transmission spectrum measured at the same time.

Resonance spectra: measured versus theory

Raw measured spectrum: Empty Beam

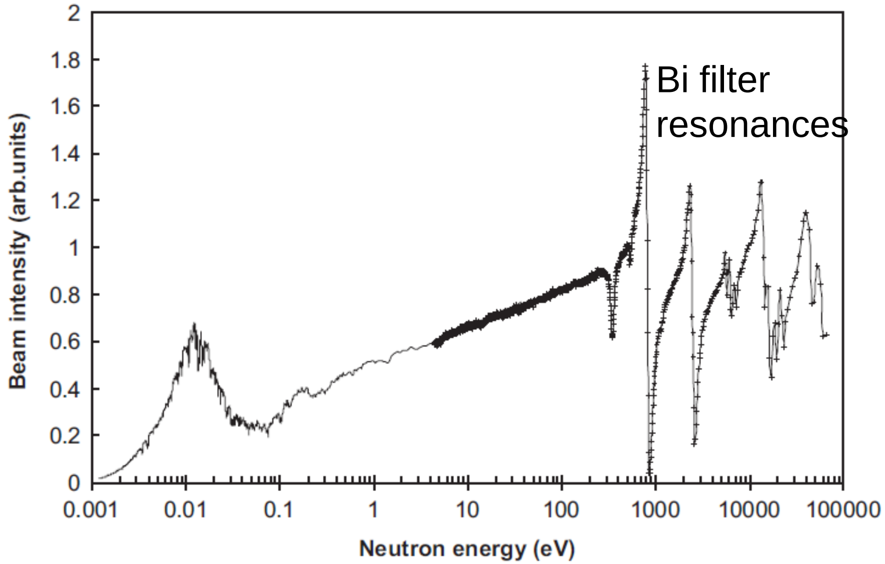

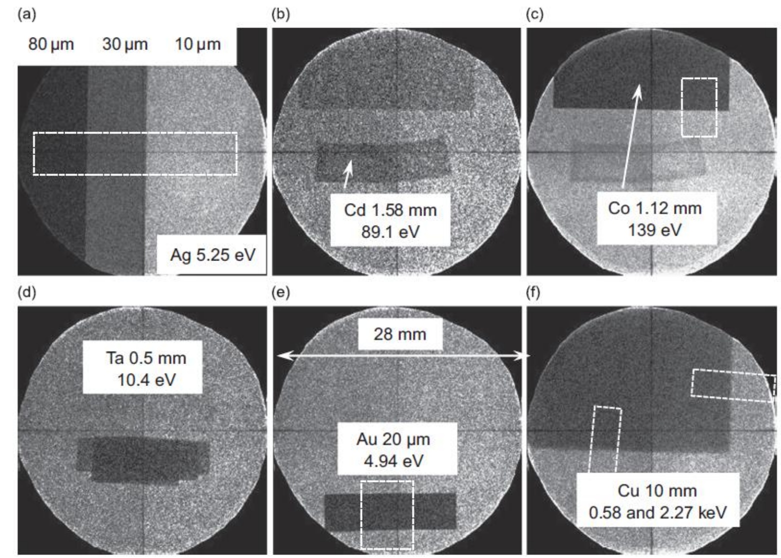

1.18 mm Ta

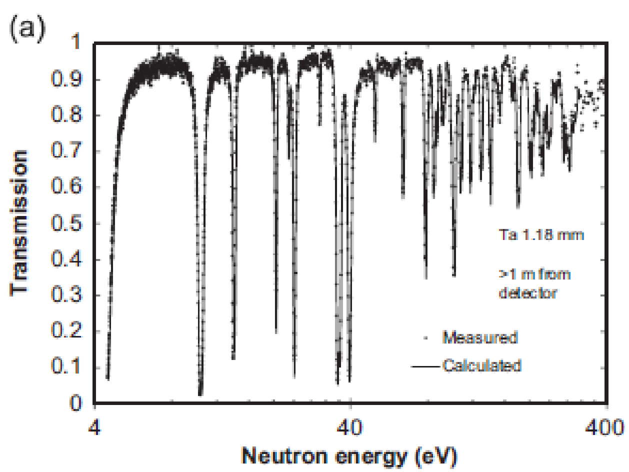

Ag: 10, 30, 80 um

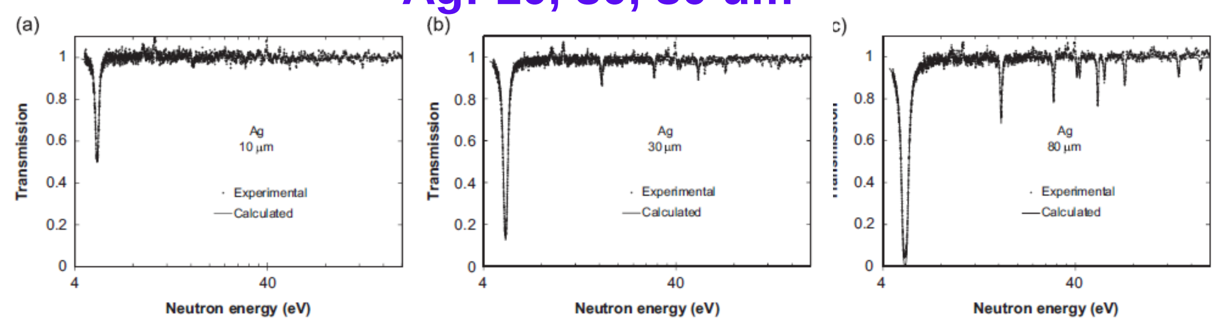

A.S. Tremsin et al., NIM A 746 (2014) 47–58

Studies of geological samples

Single crystal Gold samples

Only grow naturally. Cannot be reproduced in the lab.

Scientific Reports **7** (2017) 40759

Single crystal Gold samples: thermal neutrons

Thermal transmission image: full spectrum integrated

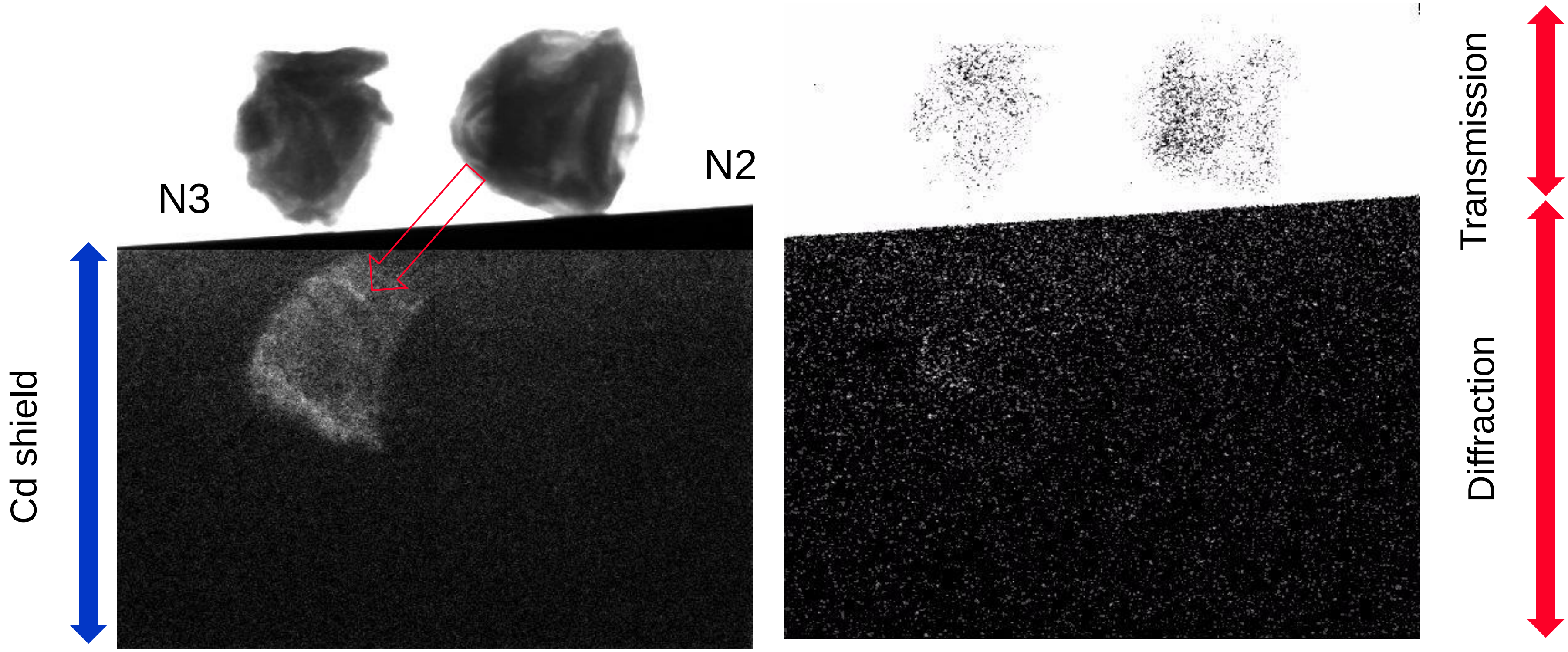

Scientific Reports **7** (2017) 40759

Single crystal Gold samples: thermal neutrons

Thermal transmission image: full spectrum integrated

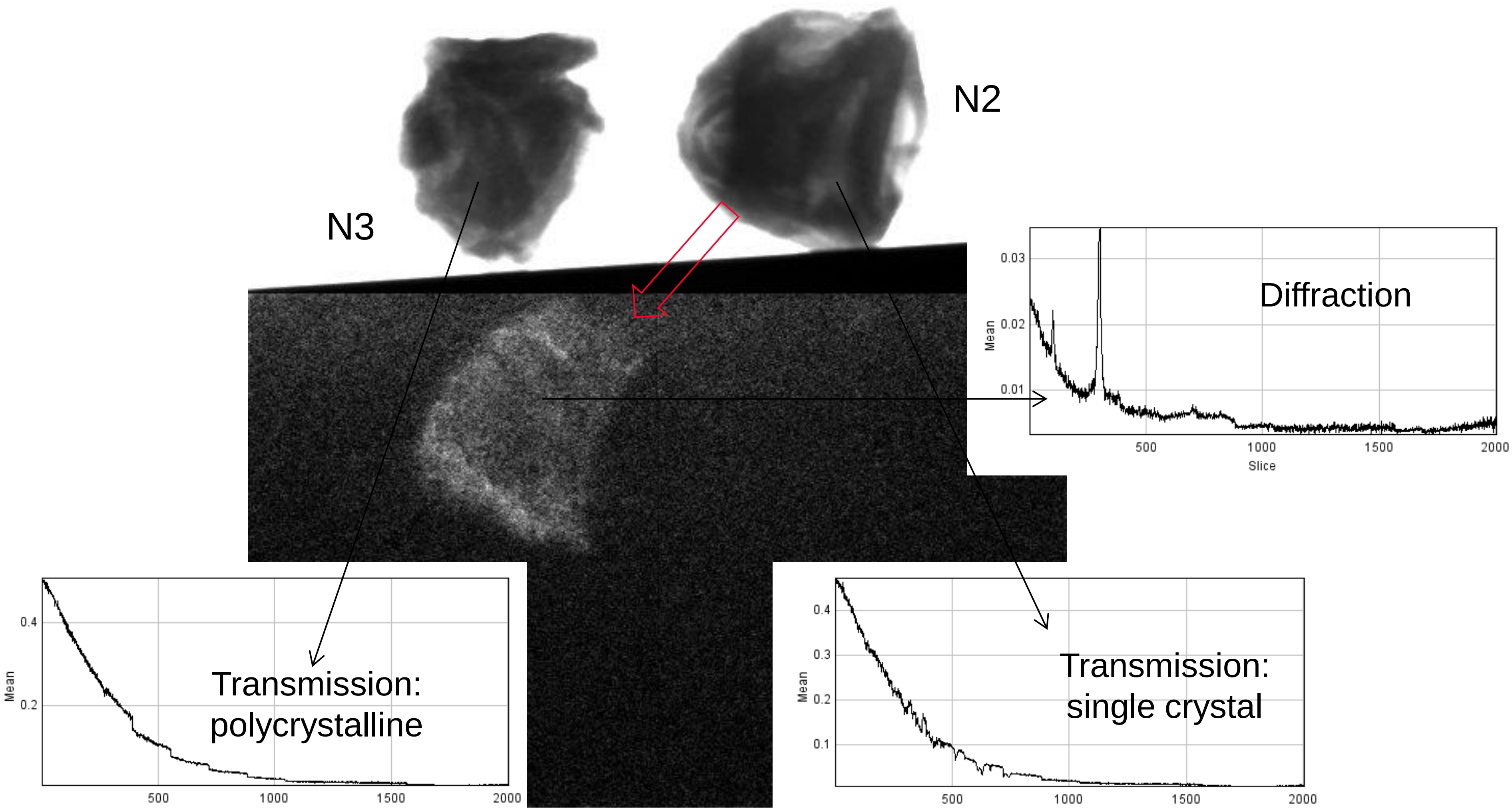

Scientific Reports **7** (2017) 40759

Single crystal Gold samples: thermal neutrons

Thermal transmission image: full spectrum integrated

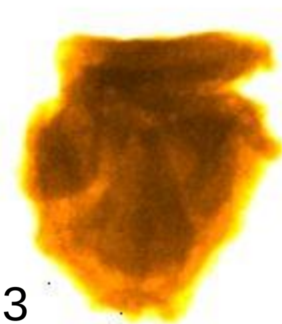
N3

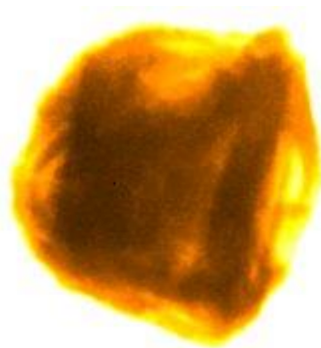
N2

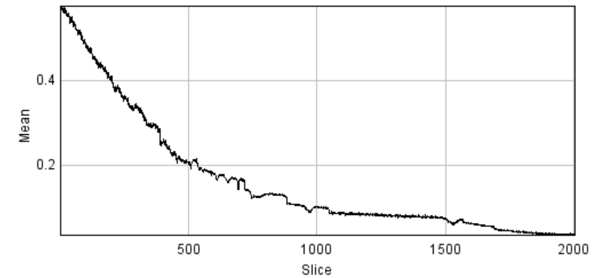

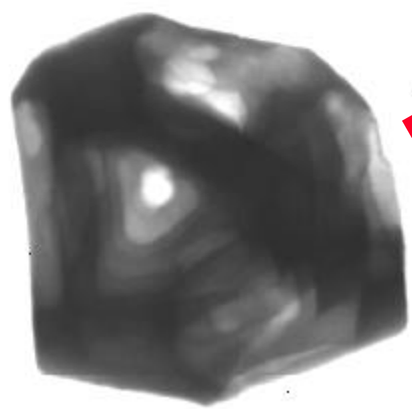
N4

N1

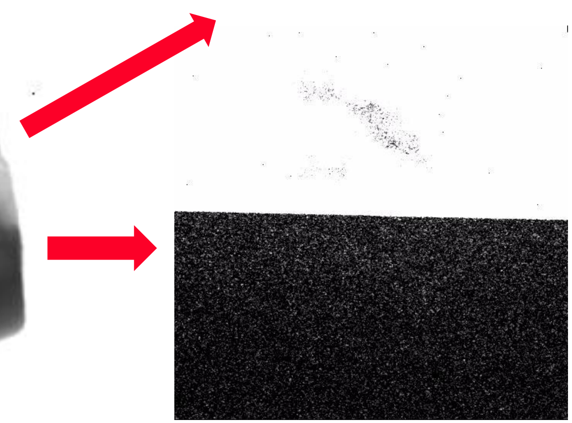

Scientific Reports **7** (2017) 40759

Single crystal Gold samples

Resonance transmission spectra

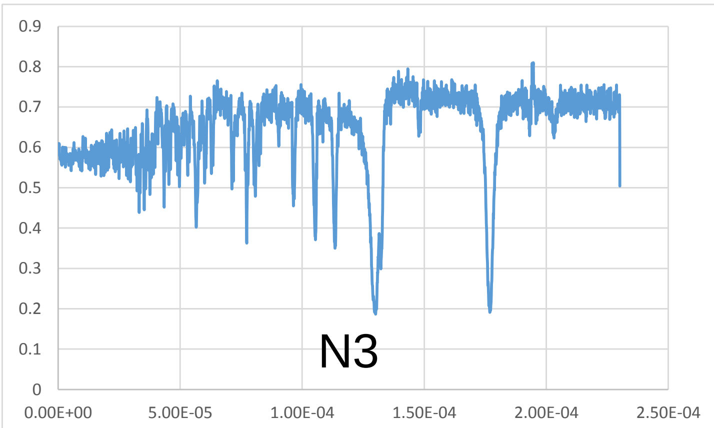

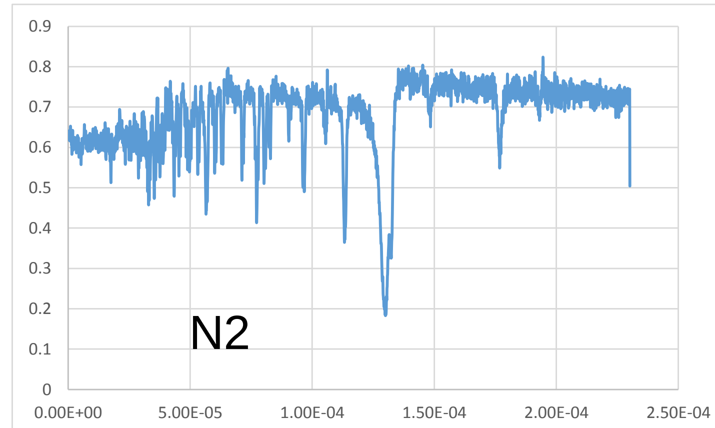

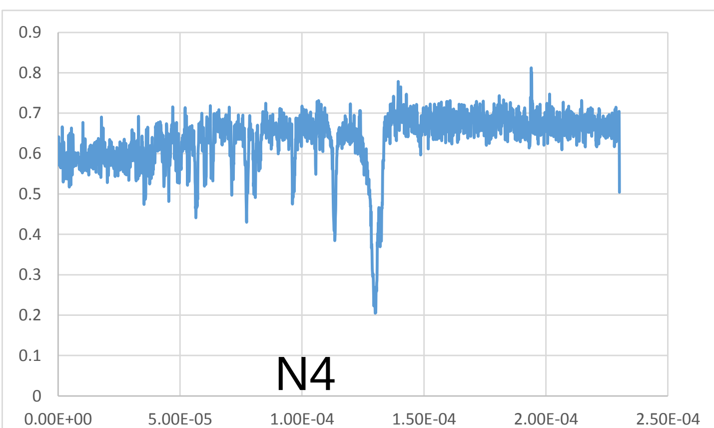

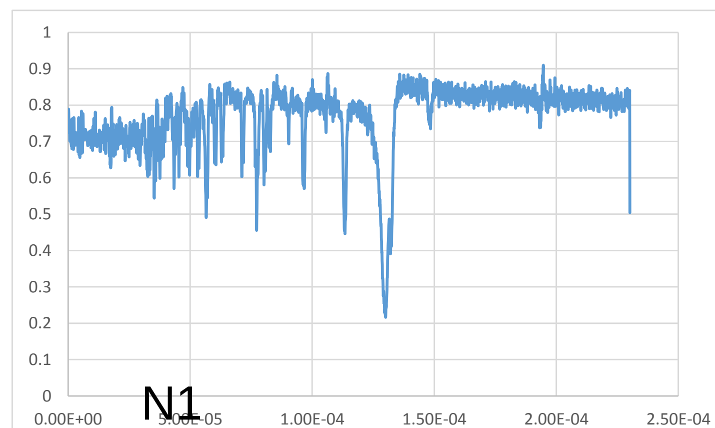

Scientific Reports **7** (2017) 40759

Single crystal Gold samples: resonances

Gold resonance energies only.

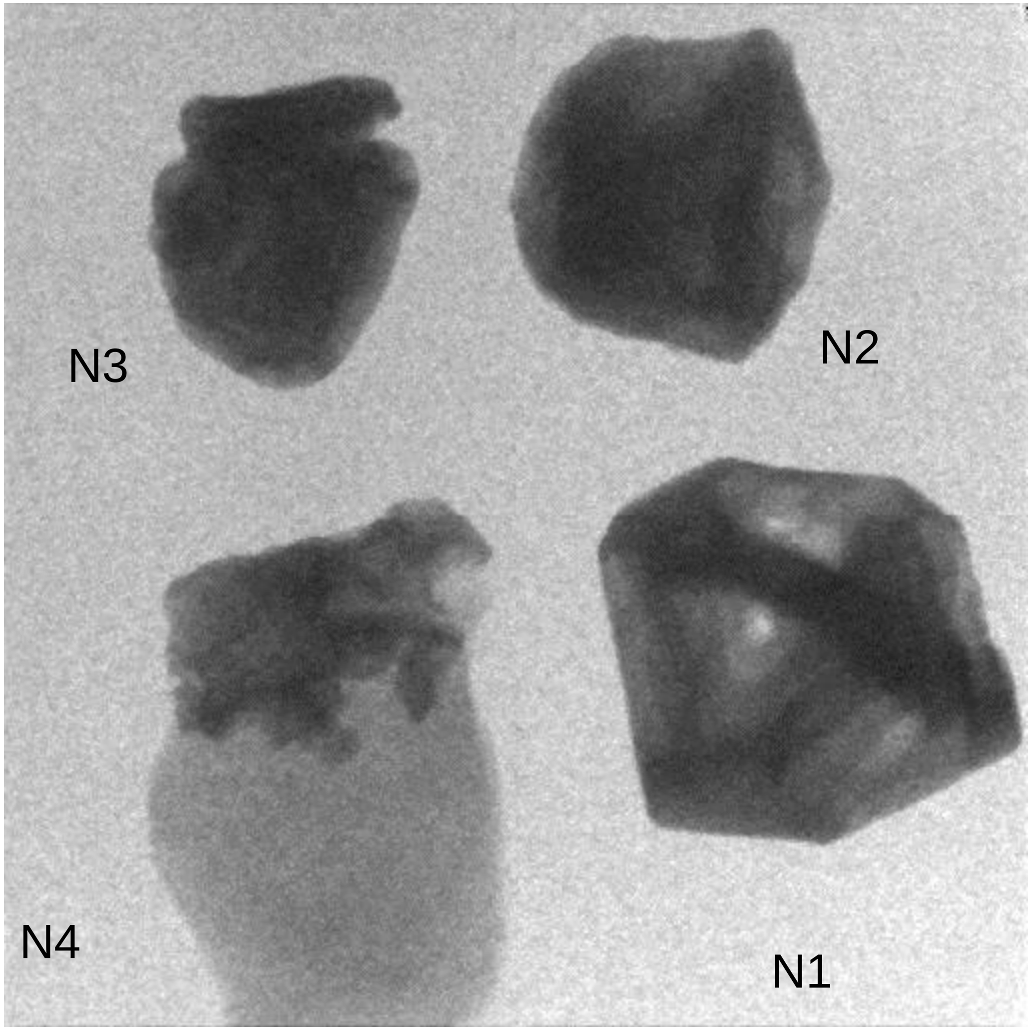

Scientific Reports **7** (2017) 40759

Single crystal Gold samples:resonances

Gold resonance energies only.

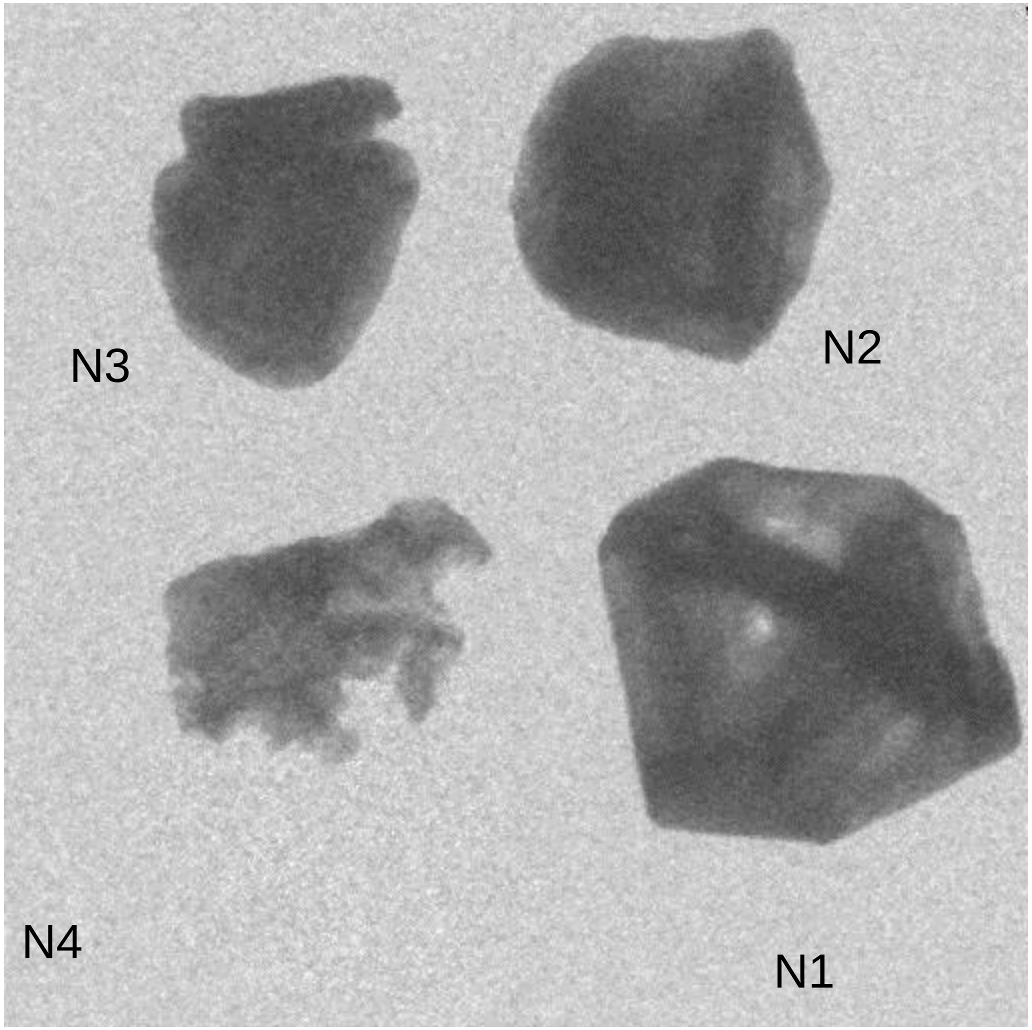

Scientific Reports **7** (2017) 40759

Single crystal Gold samples

Pd resonance energies only.

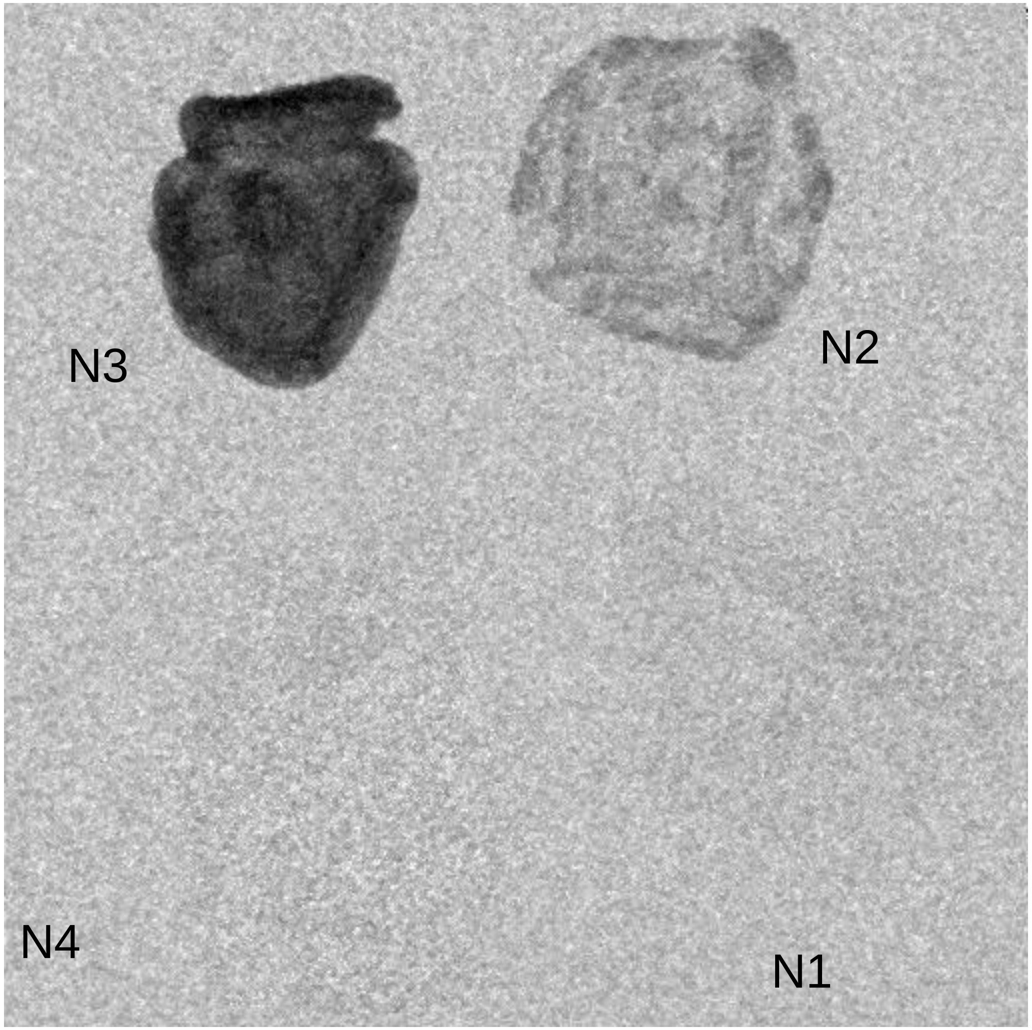

Scientific Reports **7** (2017) 40759

Remote temperature measurement through resonance spectroscopy

Remote mapping of temperature

Resonances get broader with temperature due to Doppler broadening

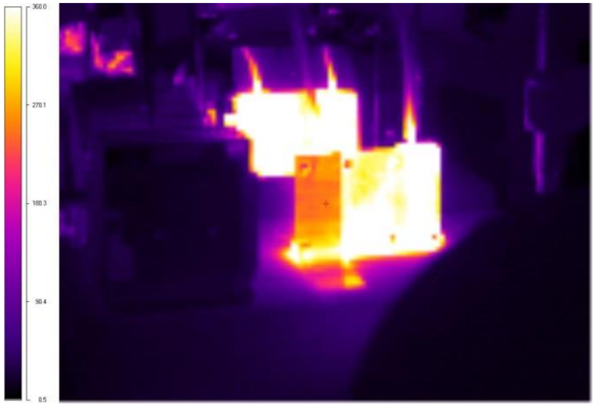

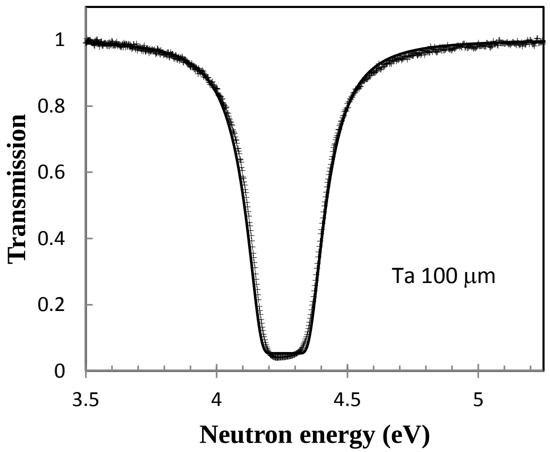

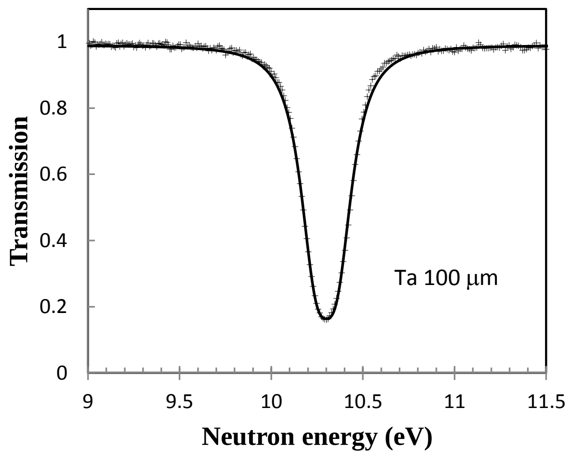

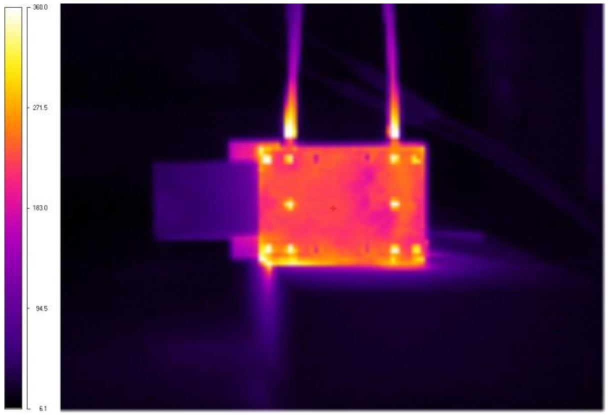

100 μm foil of Ta

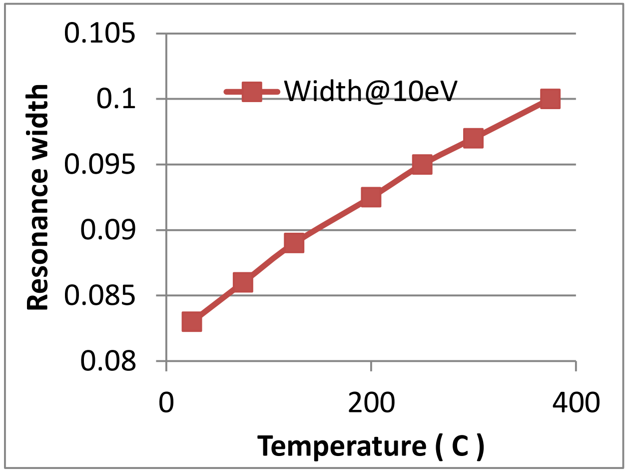

Remote temperature measurement

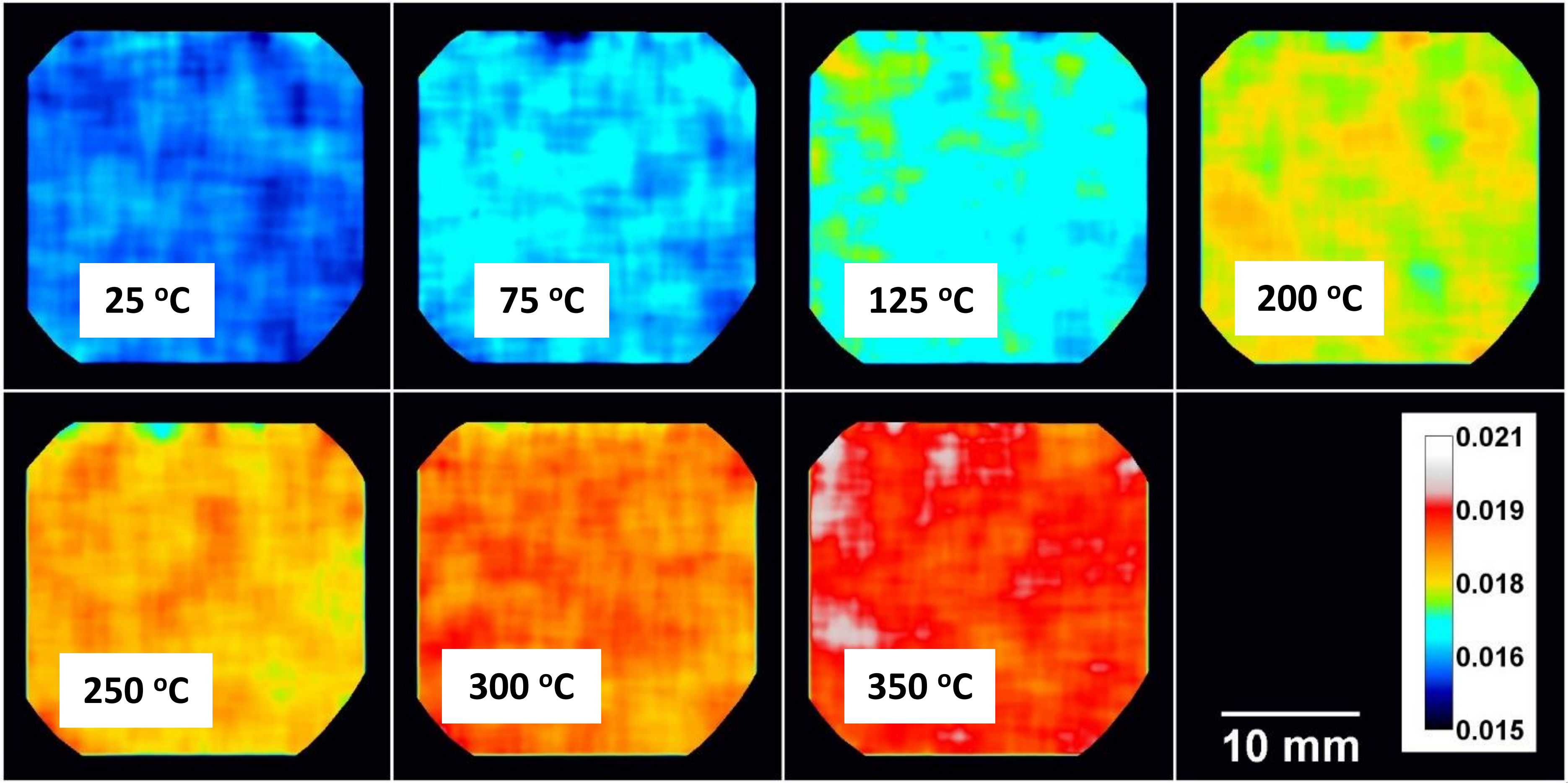

A. S. Tremsin, et al., Nucl, Instr. Meth. A 803 (2015) 15-23

Remote temperature measurement

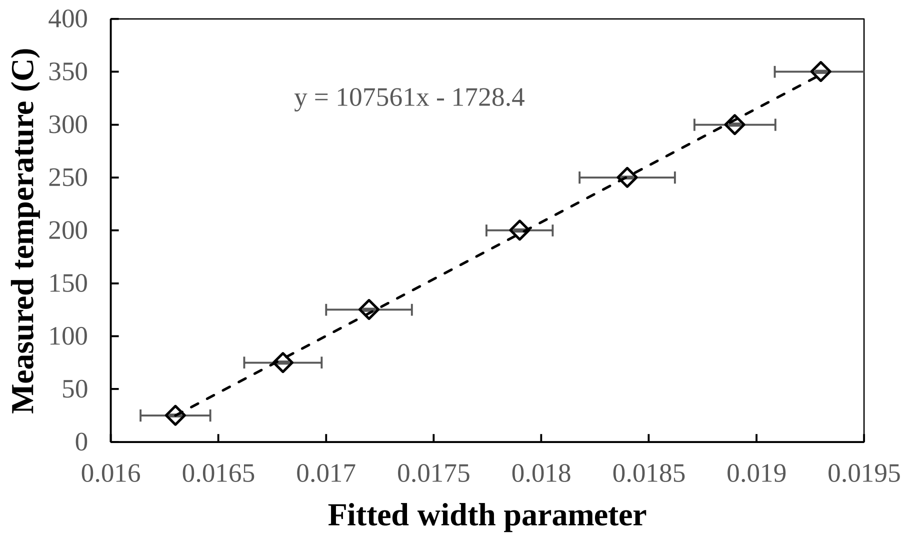

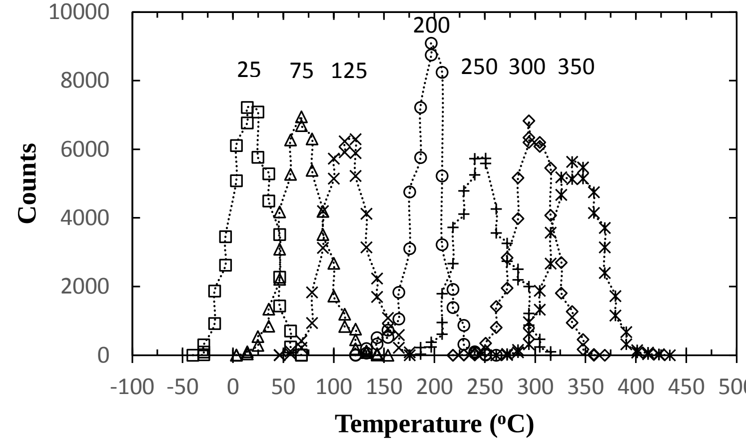

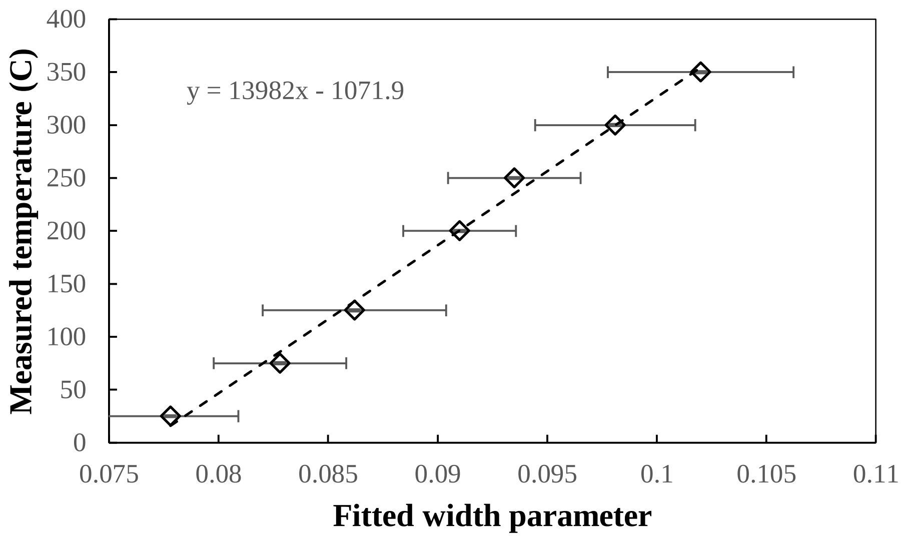

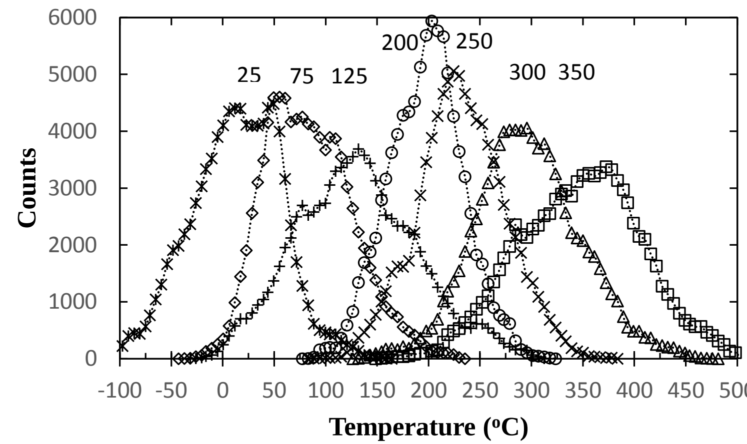

A. S. Tremsin, et al., Nucl, Instr. Meth. A 803 (2015) 15-23

Temperature gradient across the film

100 μm foil of Ta.

One side clamped at 375C and the other at the passive Al cooler block.

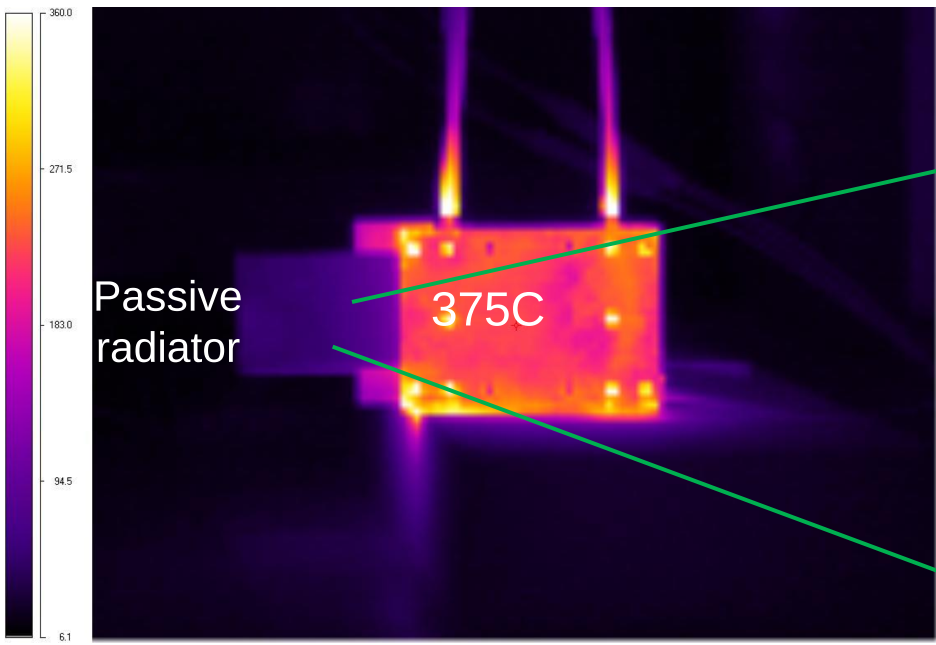

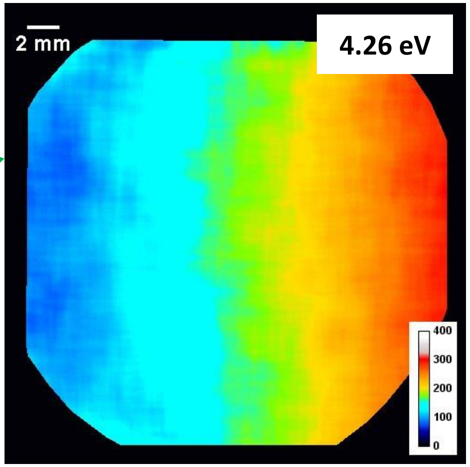

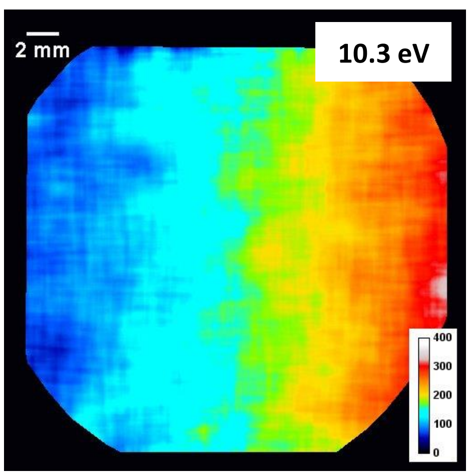

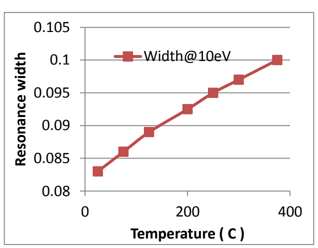

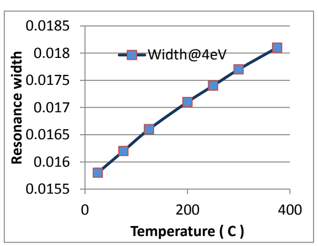

A. S. Tremsin, et al., Nucl, Instr. Meth. A 803 (2015) 15-23

Temperature gradient across the film

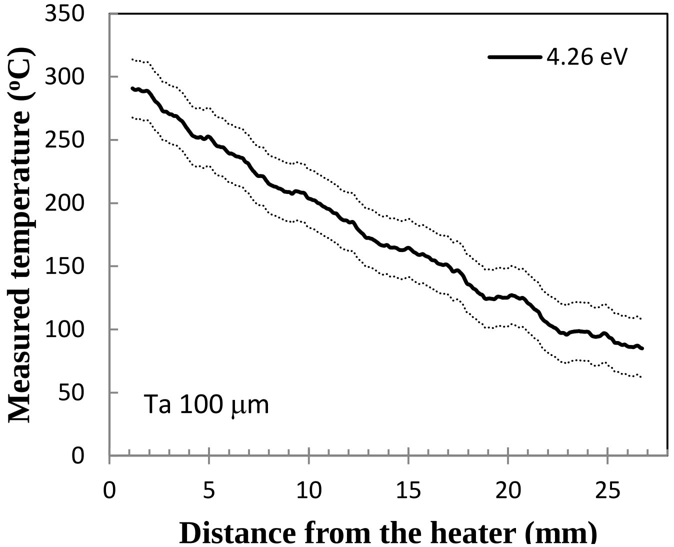

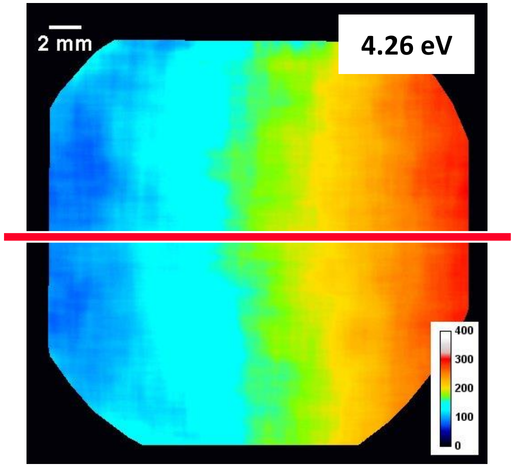

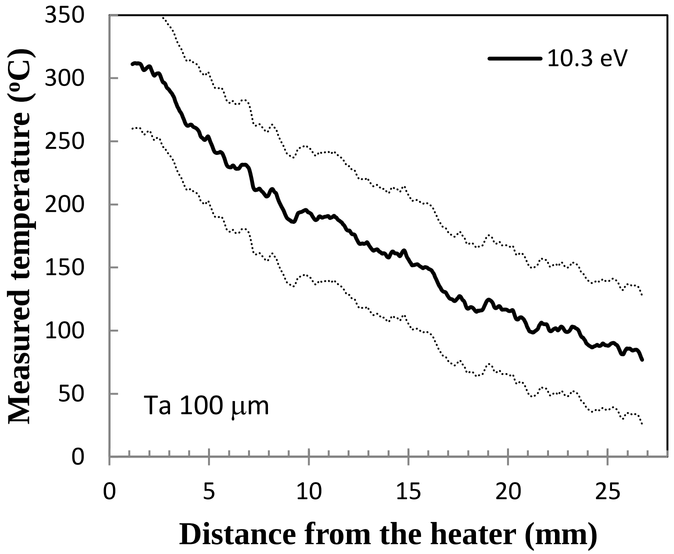

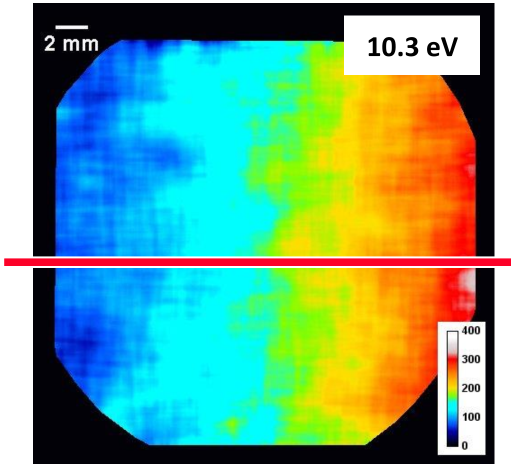

Load in Spiralock threads

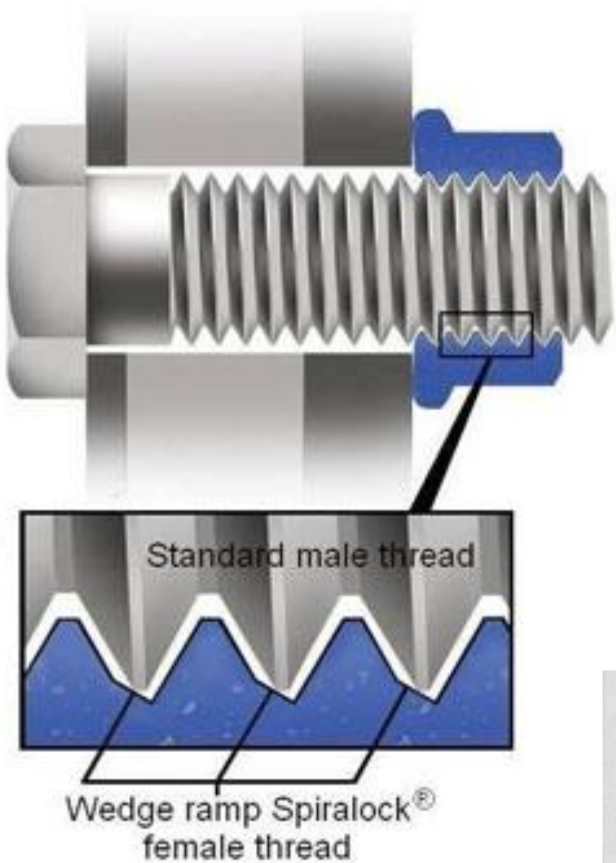

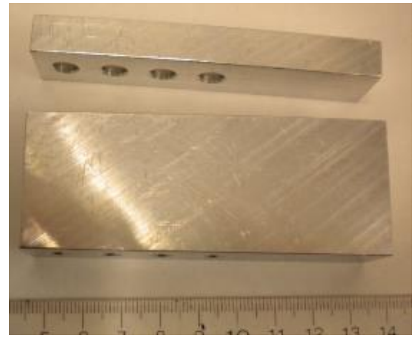

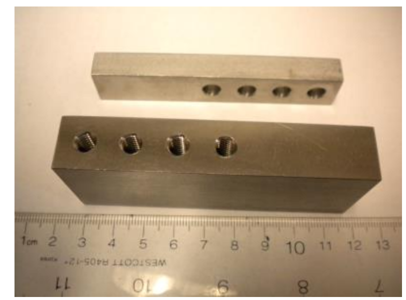

Steel screws in Al base

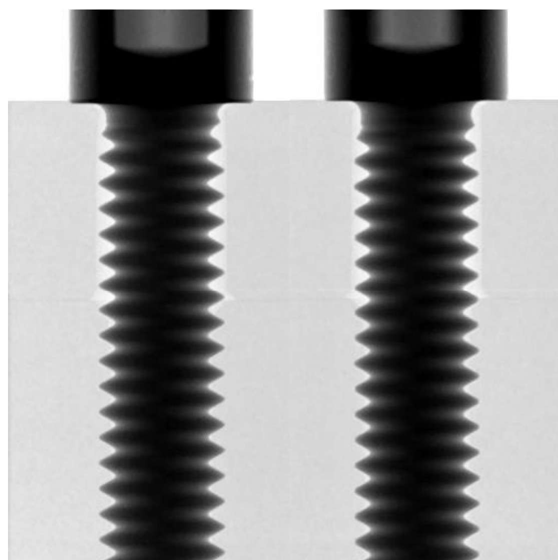

Steel screws in stainless steel

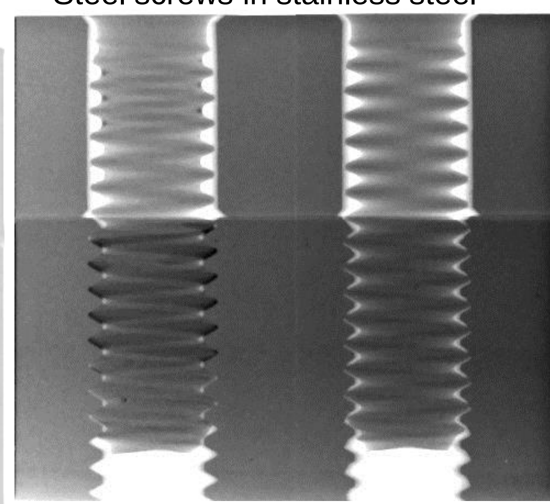

Strain **52** (2016) 548-558

Load in Spiralock threads

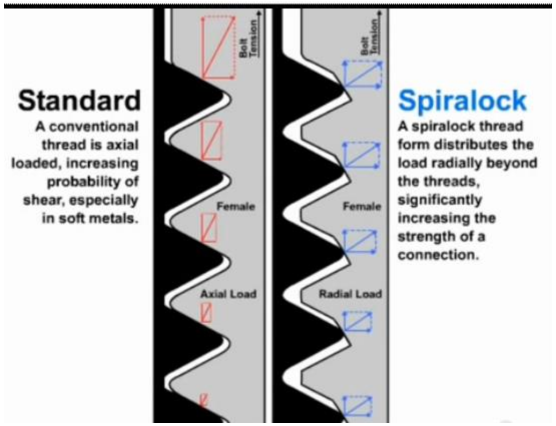

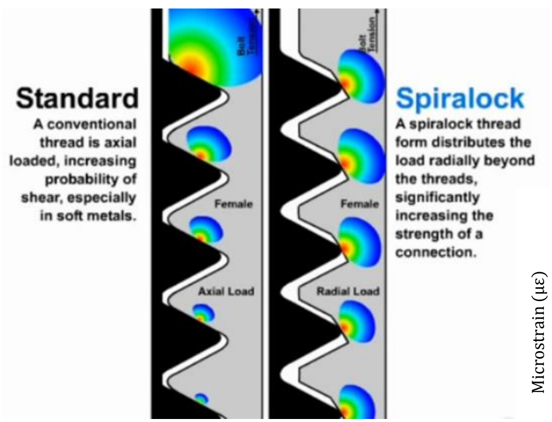

Torqued to 185 lb-in

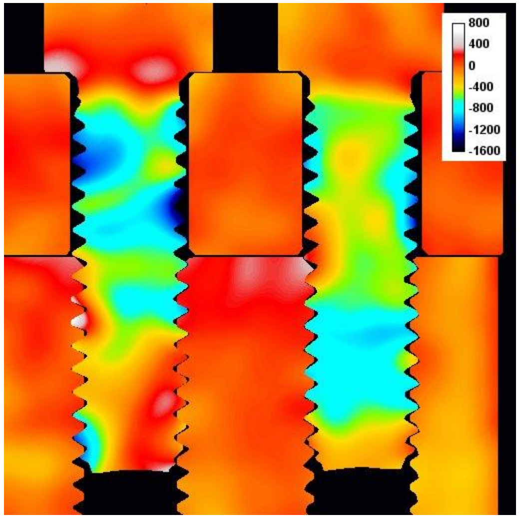

Not torqued

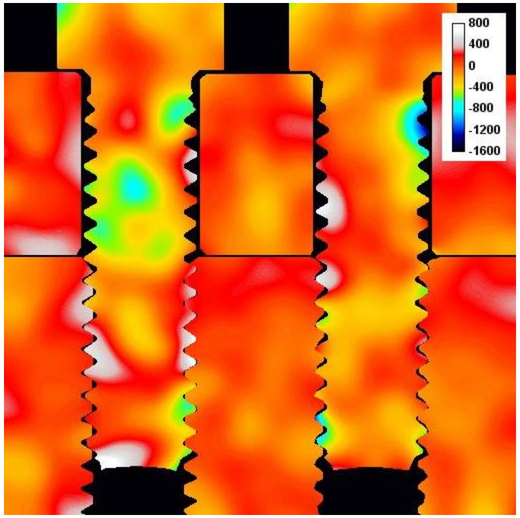

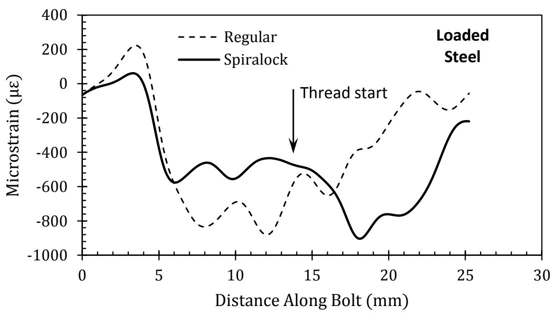

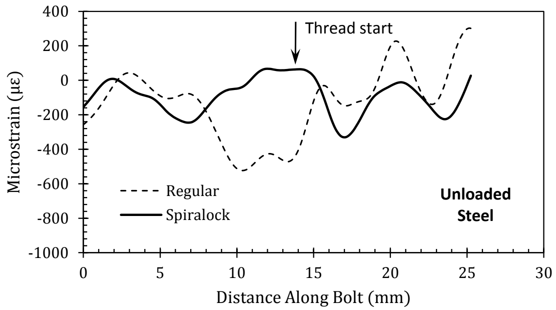

Strain **52** (2016) 548-558

In-situ studies of crystal growth

1-zone furnace calibration: temperature gradient

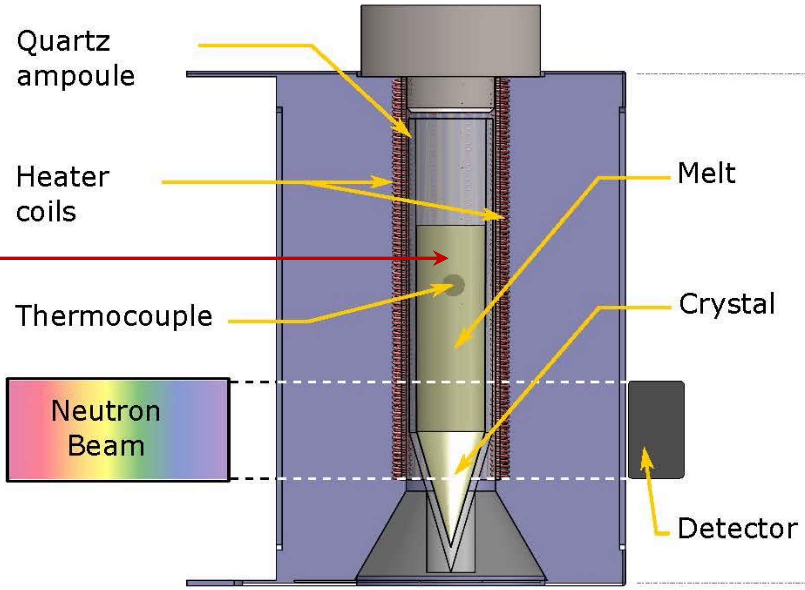

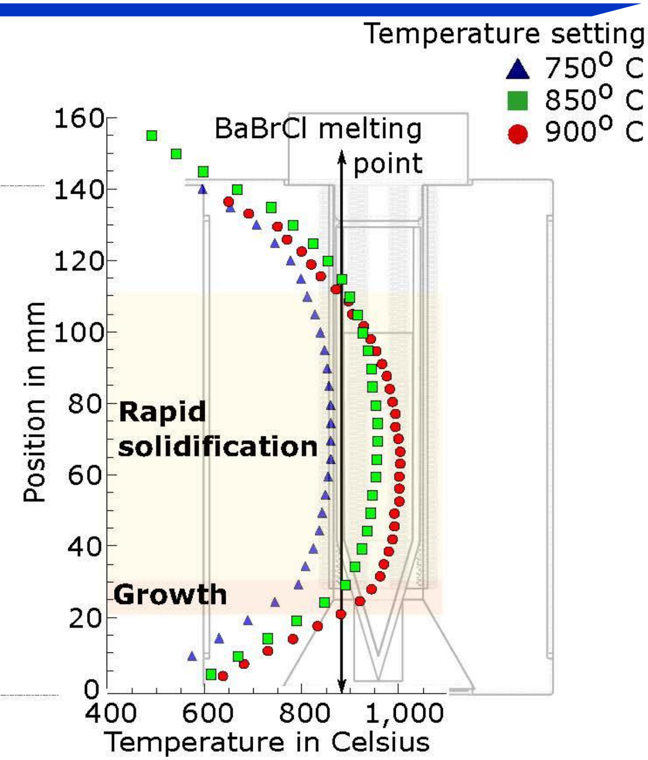

Vertical Gradient Freeze (sub-type of the Bridgman) grown at typical growth rate ~1-2 mm/hr

Charges sealed in vacuum in ~12 mm ∅ silica glass ampules

- $Cs_2LaLiBr_6$:Ce

Scientific Reports 7 (2017) 46275

Phase separation: $Cs_2LiLaBr_6$:Ce

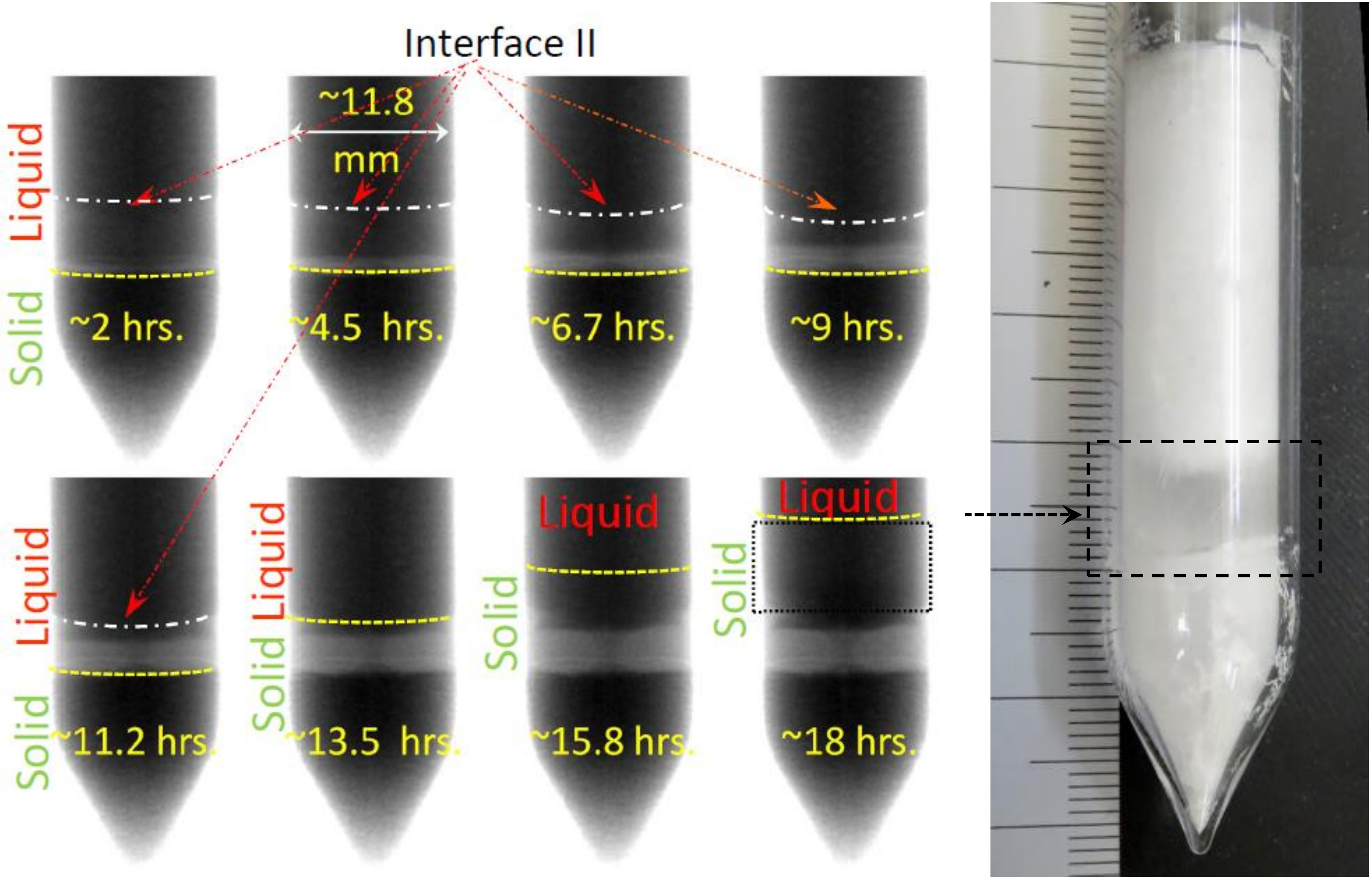

Phase separation: $Cs_2LiLaBr_6$:Ce

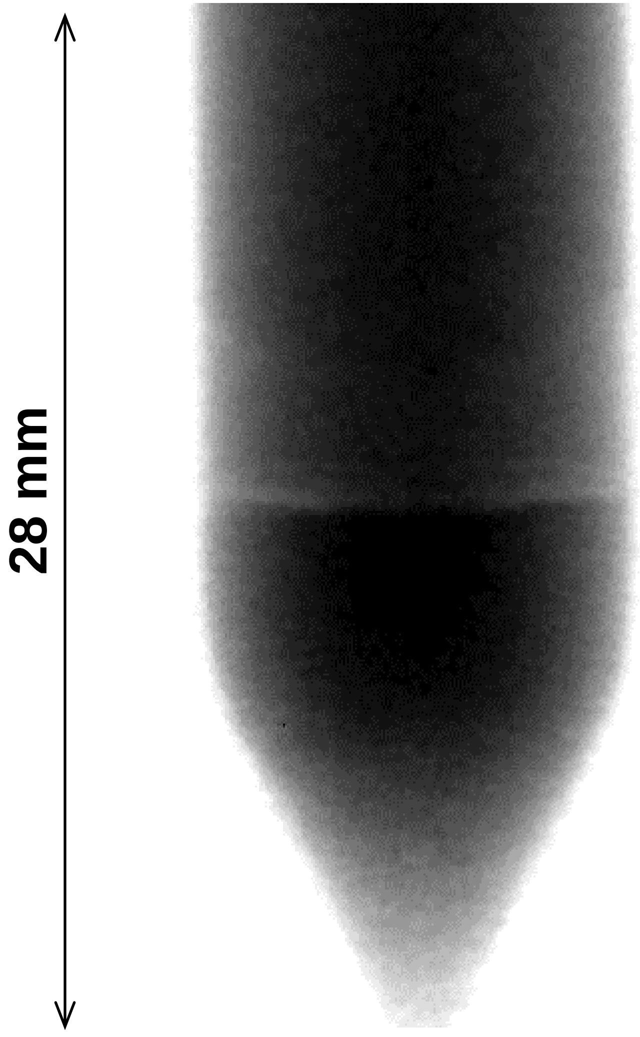

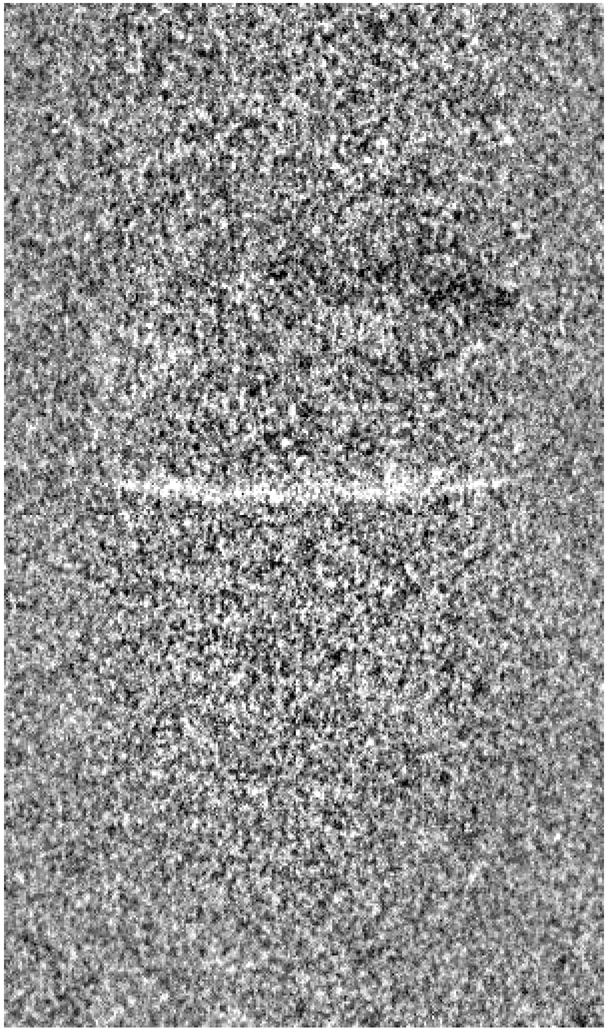

Time lapse of growth process (~40 minutes/frame)

Quantification through resonance absorption

Very challenging background quantification

Raw measured spectra

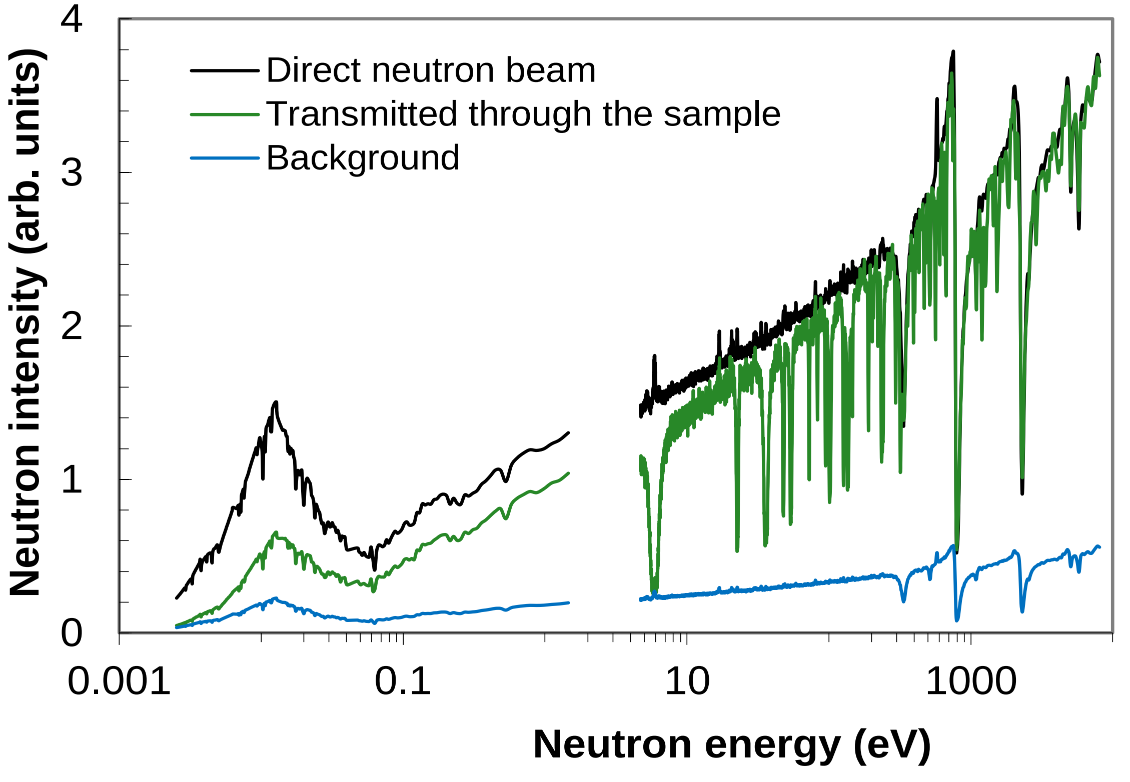

CLLB transmission

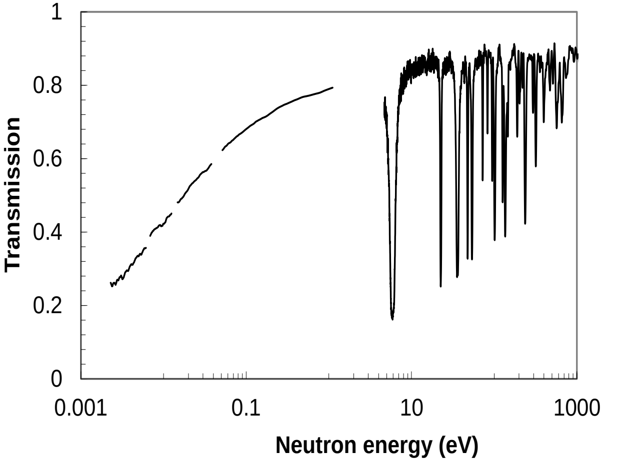

Solid/Liquid interface through diffraction imaging

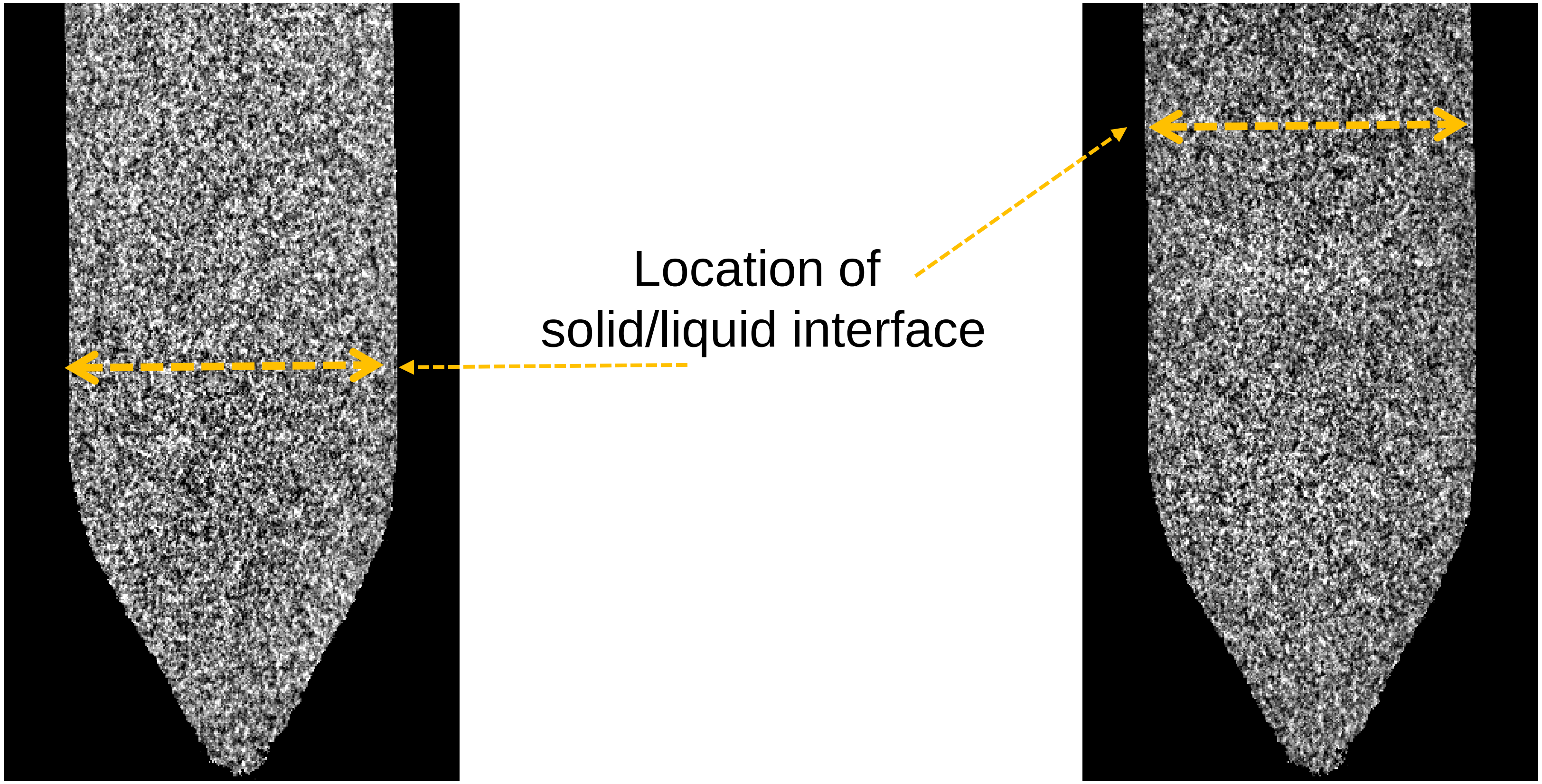

After ~ 2 hours **After ~ 18 hours**

Sensitivity to elemental composition: theory

Theoretical spectrum for a 10 mm sample

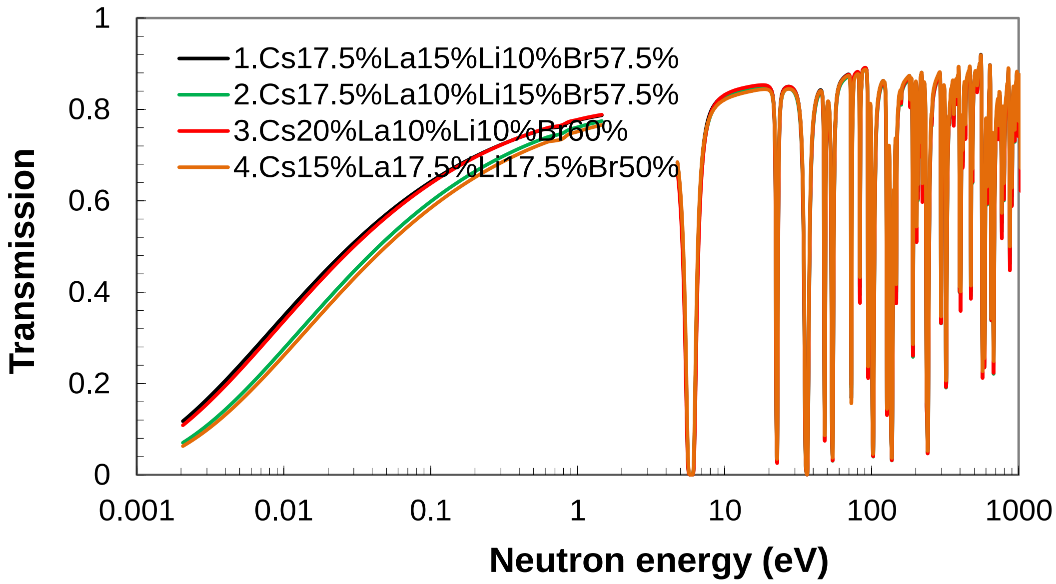

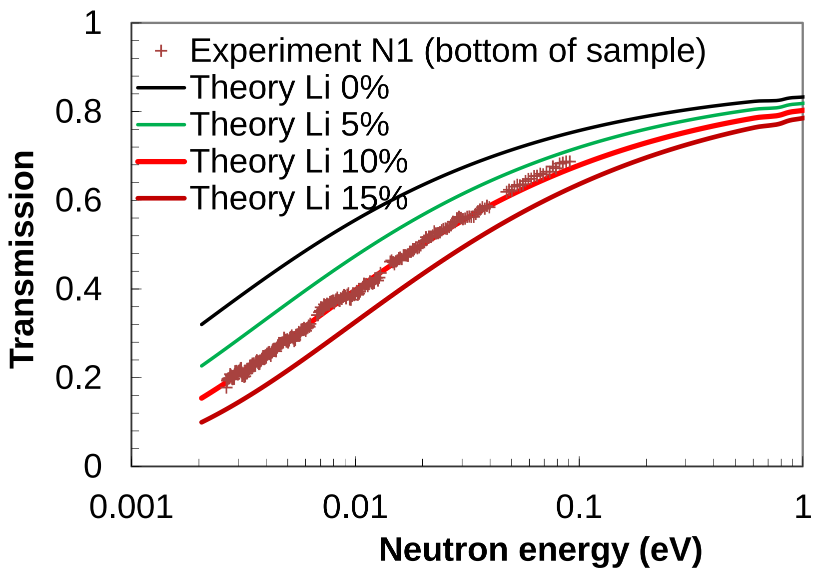

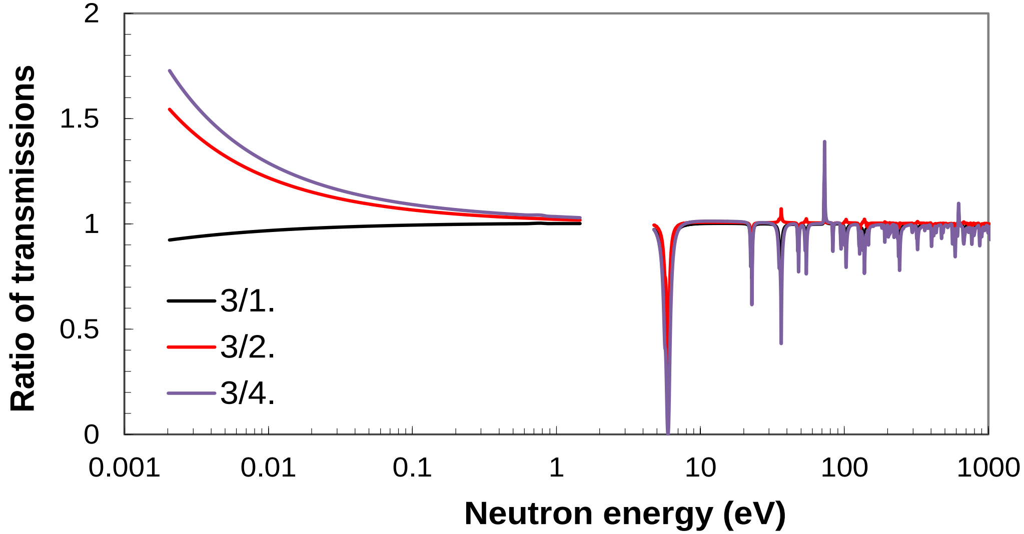

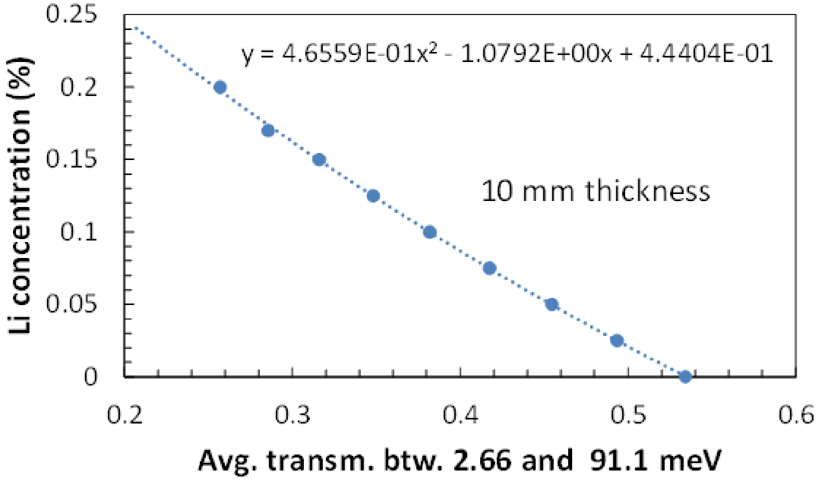

Elemental composition map: Li concentration

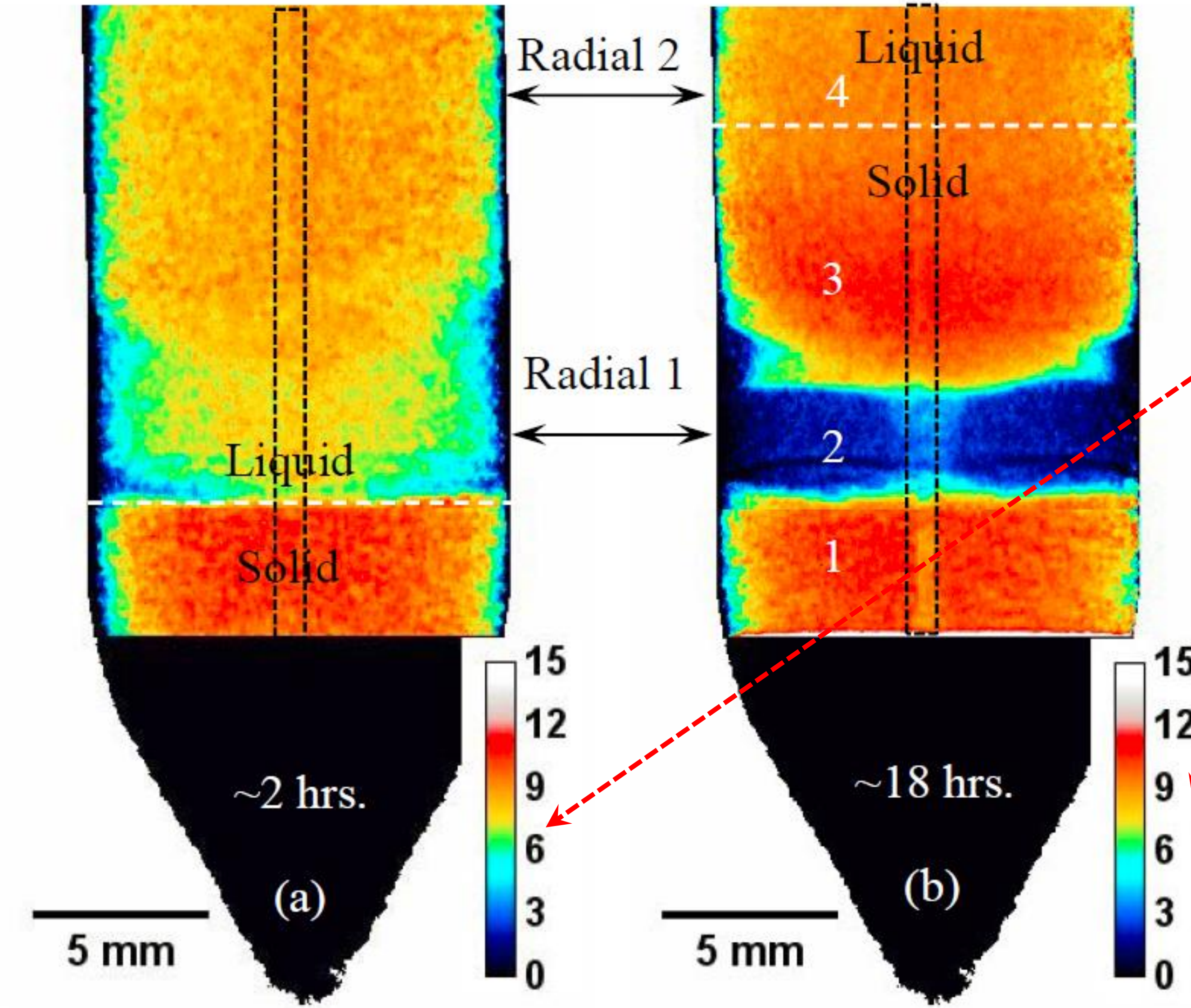

Color represents atom % concentration of Li within the ampule

A.S. Tremsin, et al., in print J. Cryst. Growth Design (2017)

Li concentration maps

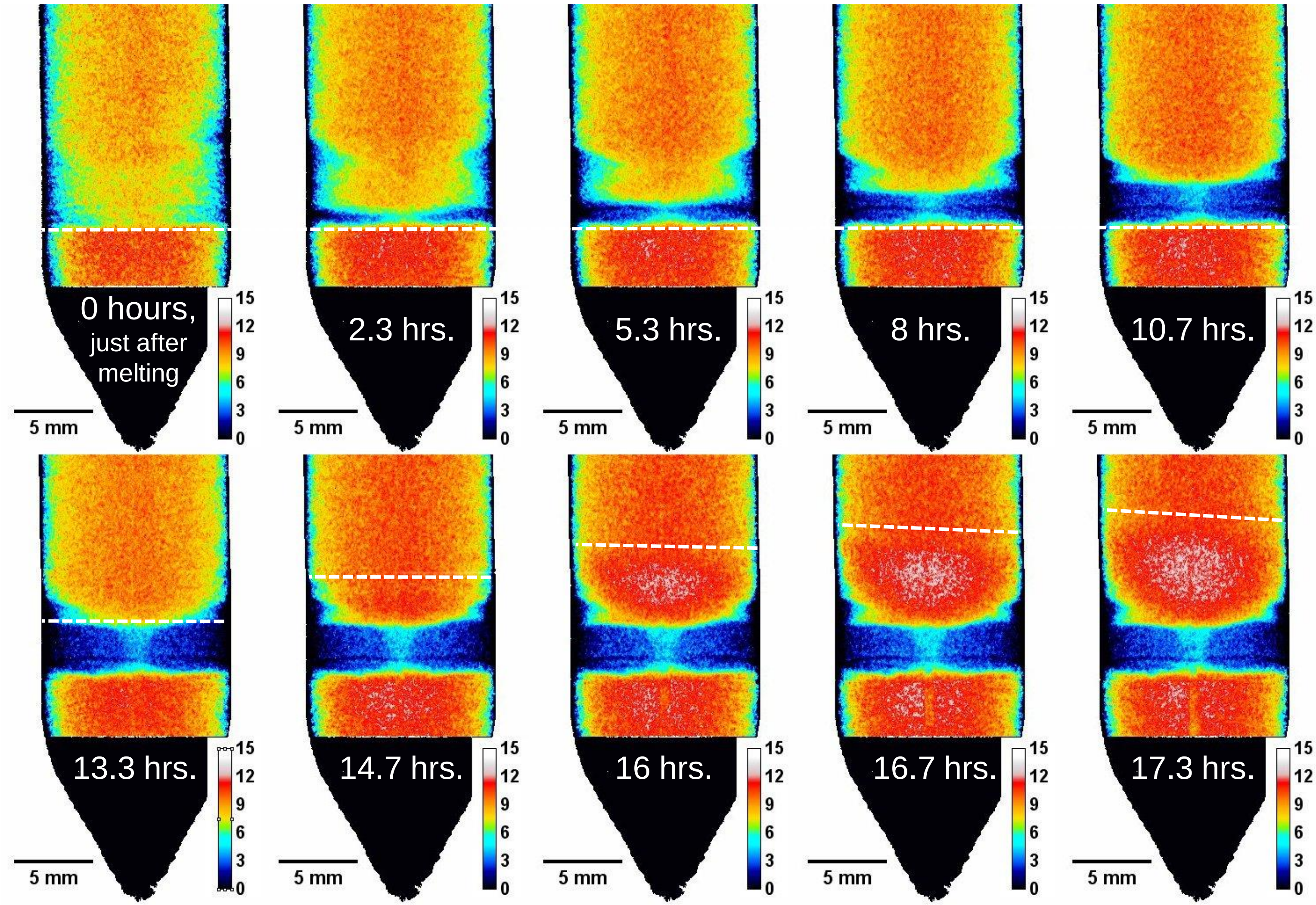

Images taken at furnace kept at constant temperature

Images taken during crystal growth through the Cs-rich area and above

Liquid/solid interface shown by dashed lines

Studies of nuclear fuels

Surrogate nuclear fuels

[Pellets :- Variable density, W inclusions, Voids ~ 5mm long , ~ 4.6 mm diameter]

Variable Density

P-dUO-09-070

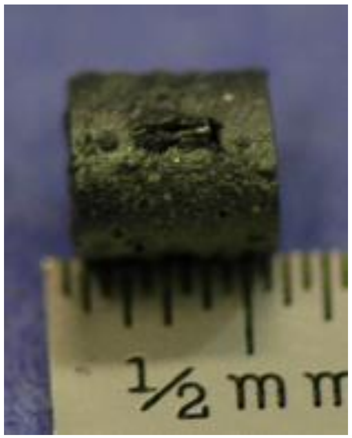

Tungsten inclusions

Wedges,
Wires (75,100,200 µm)
Particles (75,100,200 µm)

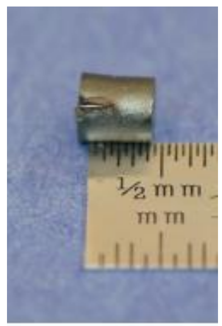

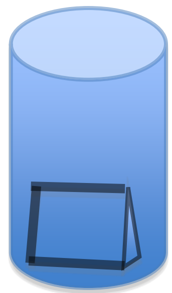

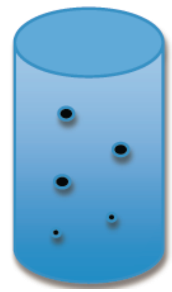

PMMA/nylon Inclusions

(result in voids)
100-400 µm

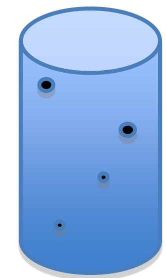

Pellet #	Mass (g)	Density (g/cc)	%TD
P-dUO-08-571	0.88745	10.32	~ 94
P-dUO-08-577	0.86811	10.11	~ 92
P-dUO-08-576	0.87310	9.74	~ 88
P-dUO-09-069	0.8282	8.57	~ 78
P-dUO-09-068	0.4916	5.32	~ 48

Pellet #	Tungsten Wedge / Wires
P-dUO-09-071	Wedge (radial) 230 to 24µm taper
P-dUO-09-070	Wedge (longitudinal) 319 to 49µm taper
P-dUO-09-073	Wires (longitudinal) 75,100,200µm x ~3-4mm length
P-dUO-09-075	Wires (transverse) 75, 100, 200µm x 3-4 mm length
P-dUO-09-072	Particles dispersed 75 to 200µm
P-dUO-09-079	Wires same length as diameter in 75, 100, and 200µm sizes

Pellet #	PMMA Particles/ Wires
P-dUO-09-077	Line Voids produced by Fishing line 210µm diameter in center in longitudinal direction
P-dUO-09-080	Ideally spherical voids produced by PMMA polymers
P-dUO-09-076	Line Voids produced by Fishing line 210, 270, 380µm diameters in transverse direction (radially)
P-dUO-09-078	Line Voids produced by Fishing line 210, 270, 380µm diameters in longitudinal direction

Journal of Nuclear Materials **440** (2013) 633

Epithermal neutron imaging (LANL)

Scan through energy slices

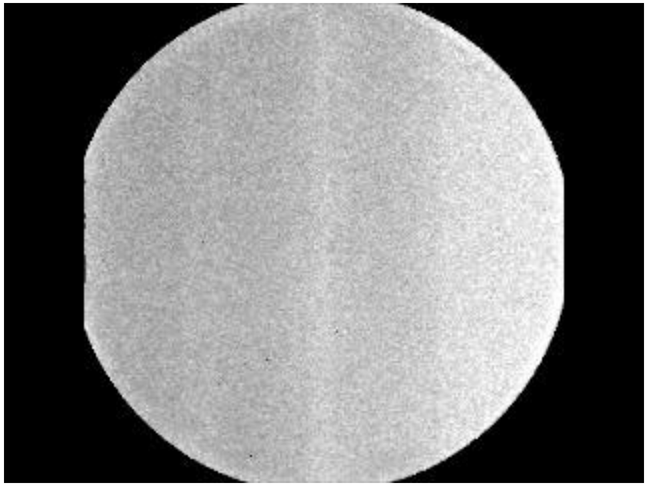

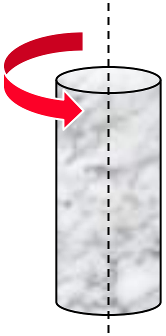

Sample rotated by
90 degree

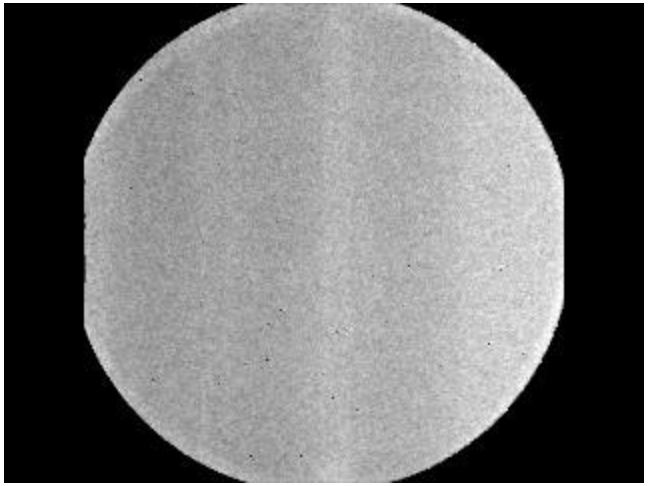

U – resonance slices

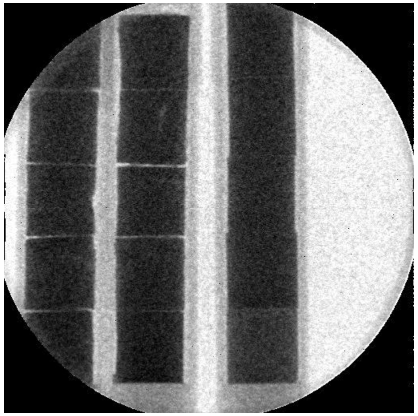

W – resonance slices

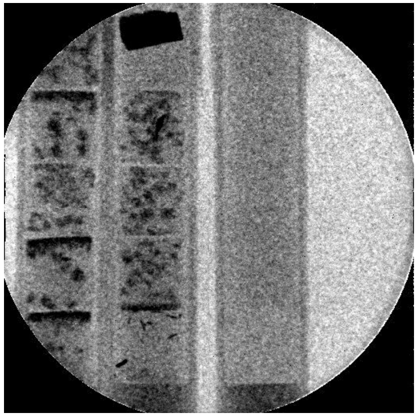

U – resonance slices

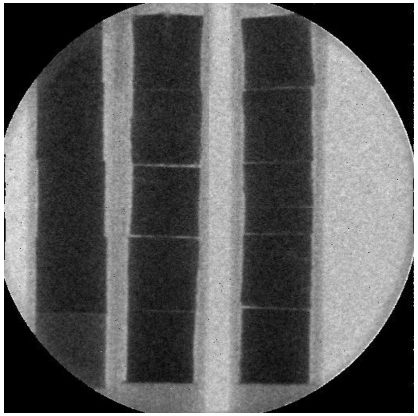

W – resonance slices

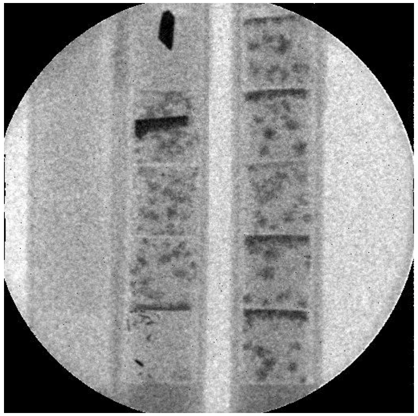

Journal of Nuclear Materials **440** (2013) 633

Thermal neutron radiography (LANL)

0 degree rotation

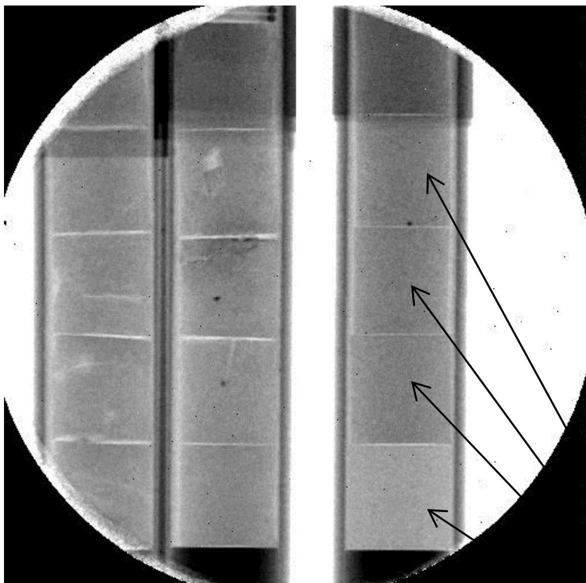

45 degree rotation

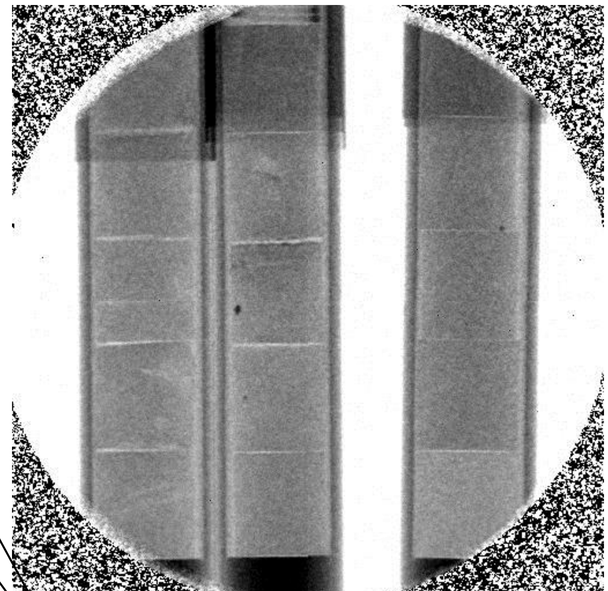

90 degree rotation

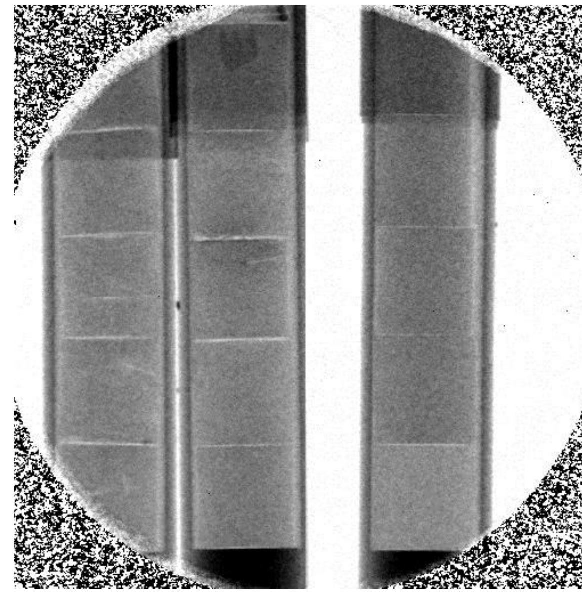

Voids and cracks are visible

Varied density pellets

Journal of Nuclear Materials **440** (2013) 633

Multi-modal imaging in one measurement

Thermal nRad	U resonance	Ratio of nRad to W resonance	Ratio of U/W resonances

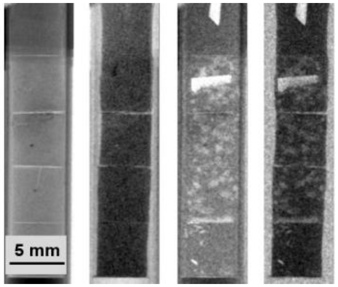

Summary

- Neutron energy-resolved imaging enable unique non-destructive studies of polycrystalline and single crystal materials.
- It can provide complimentary information to other methods.
- Both crystallographic properties such as texture, phase composition and strain can be mapped simultaneously with elemental composition within the bulk of relatively thick samples.
- Elemental-specific imaging of various materials can be performed in one measurement.
- In-situ studies of crystal growth/alloying can be performed

This work was supported in part by NASA, DOE, NSF, NIH and NNSA.

The work on MCP/Timepix detector was done within the Medipix collaboration.

Thank you for your attention!

Imaging of gases within high-Z materials:

Xe and Kr gasses in a steel pipe at pressure ~100 Psi

Setup 3: Xe gas and one fuel assembly

Xe in a steel pipe installed next to two fuel pin assemblies

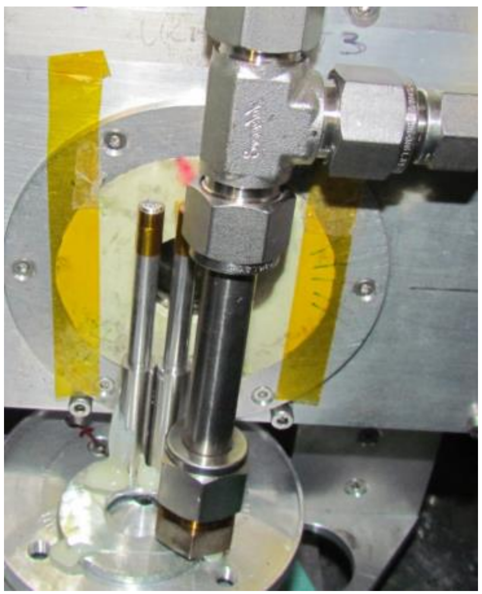

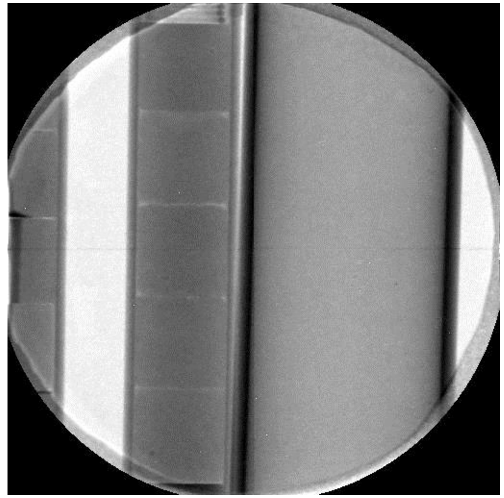

Full spectrum transmission image

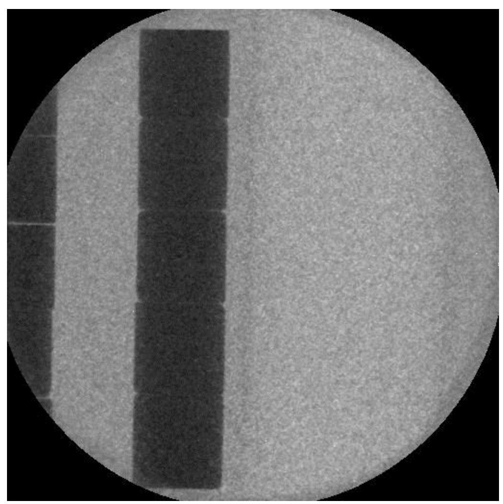

Resonance energy of U

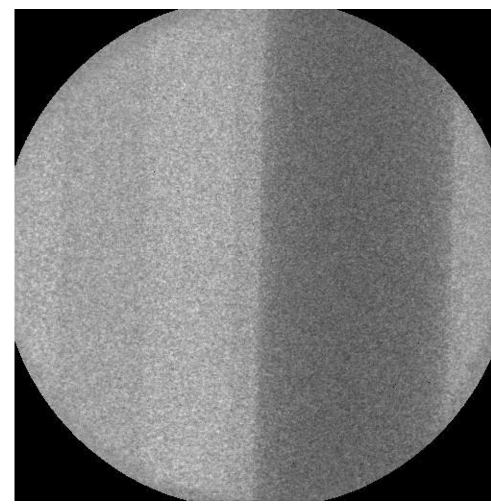

Resonance energy of Xe

AIP Advances 7 (2017) 015315

Setup 3: Xe gas and one fuel assembly

Xe in a steel pipe installed next to two fuel pin assemblies

Transmission spectrum at various Xe thicknesses

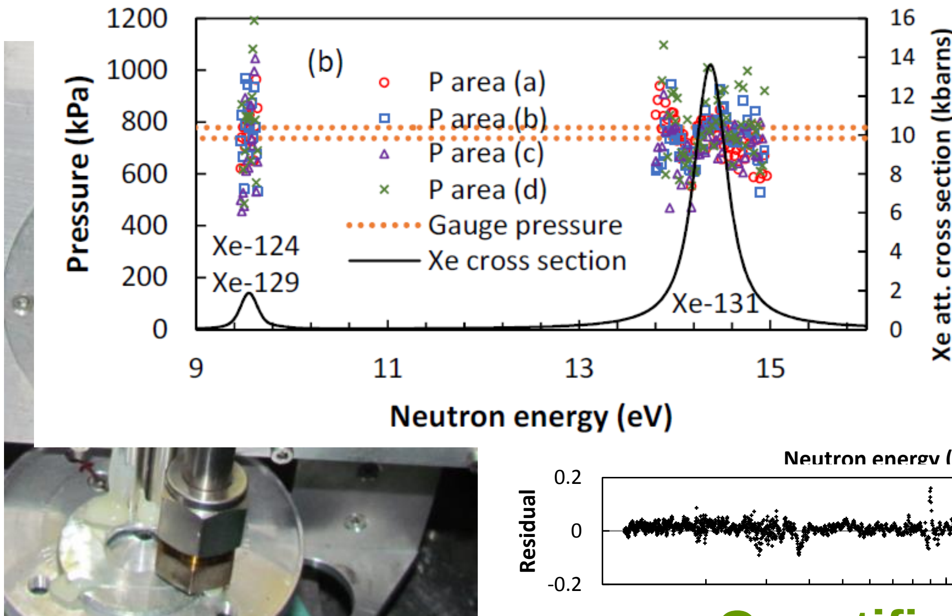

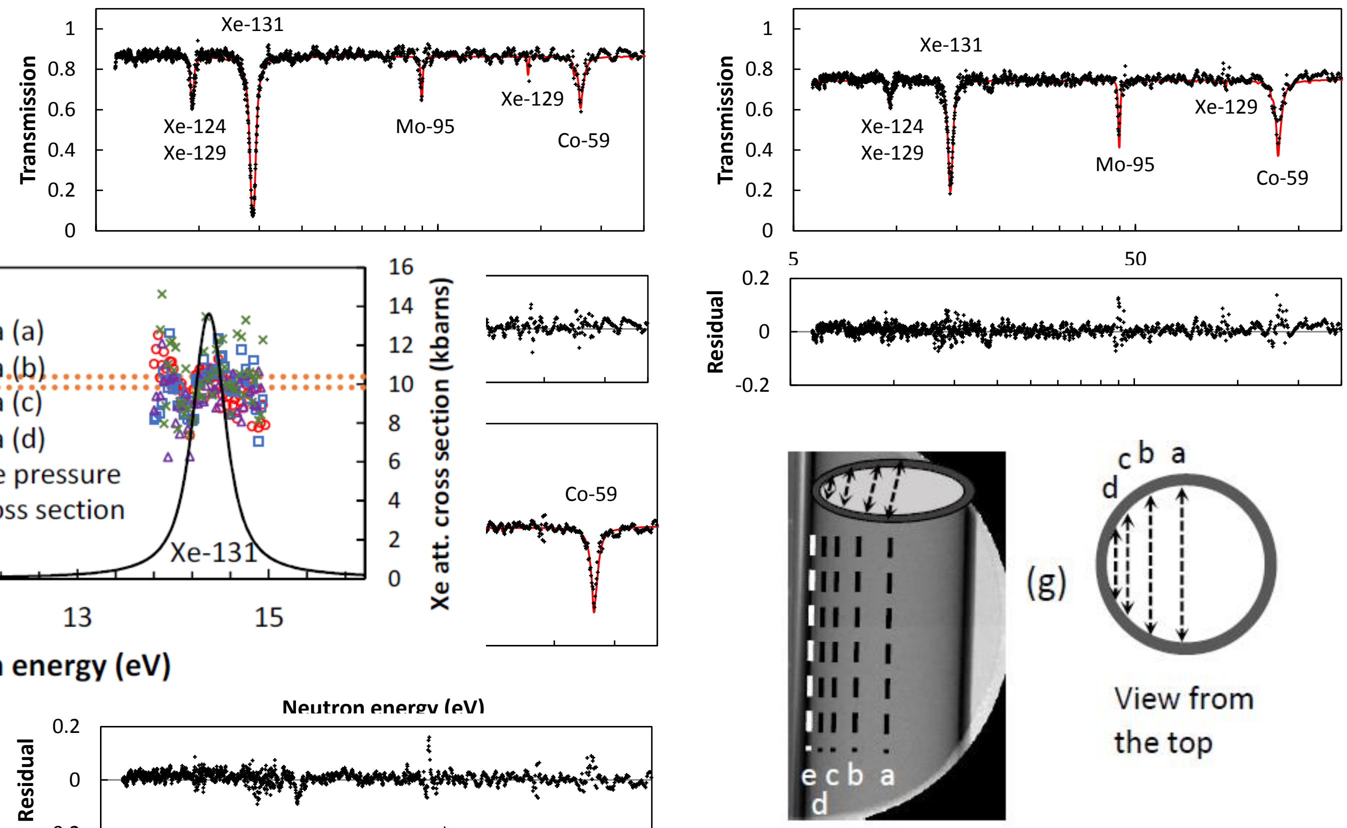

AIP Advances 7, 015315 (2017)

Quantification allows measurement of number of gas molecules.

For given geometry and temperature – can measure gas pressure

Element specific imaging

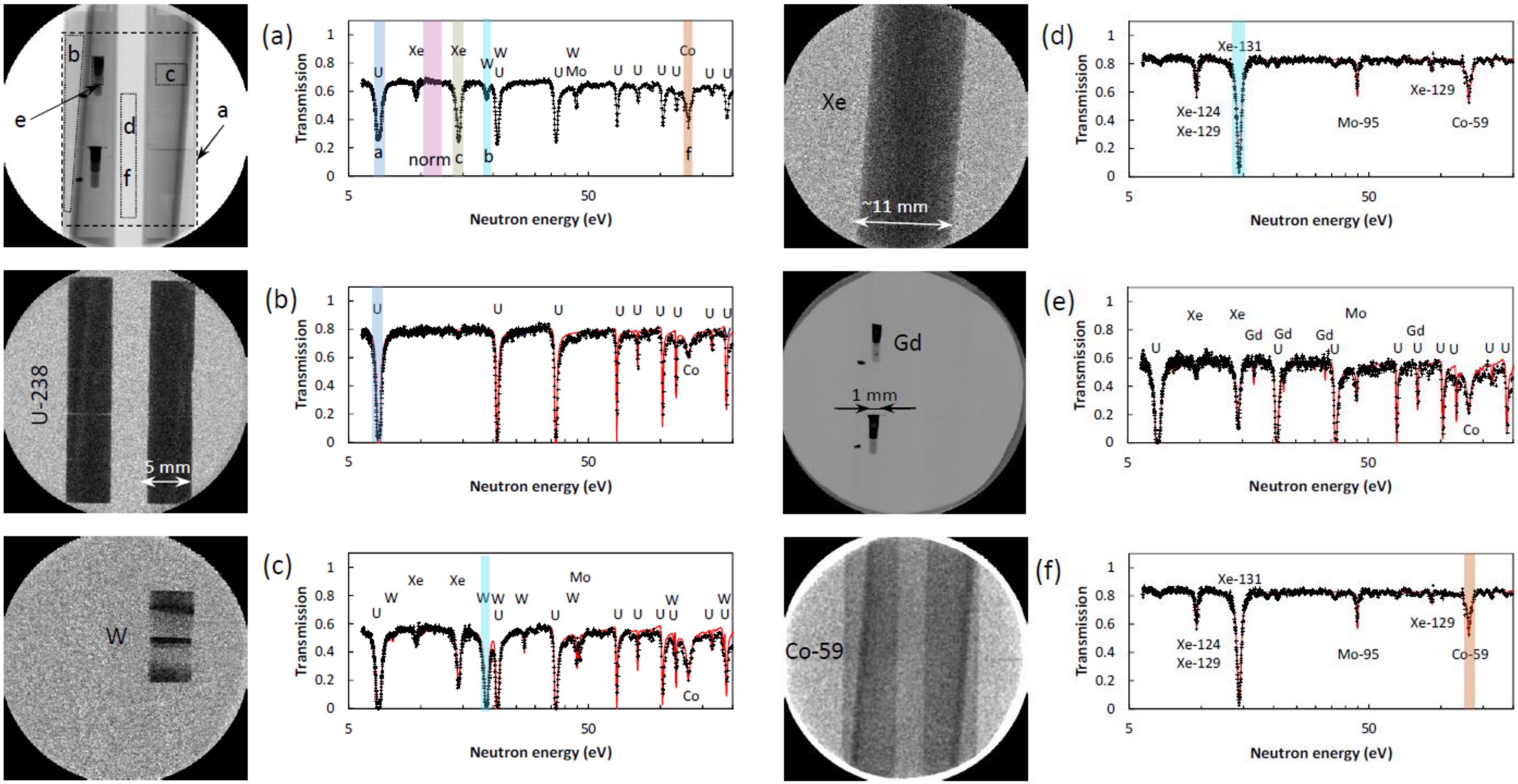

All images are measured in one experiment!

AIP Advances 7, 015315 (2017)

Dissimilar welds: SS to Titanium; Al to Steel

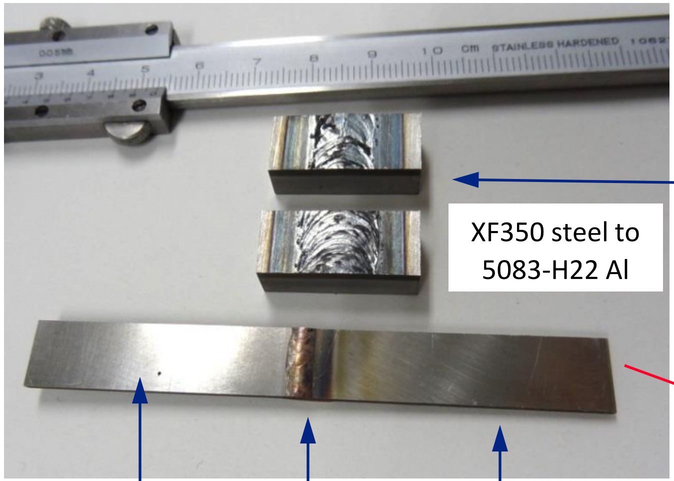

Steel to Al:
laser welded

Steel

Copper welding interface

Ti

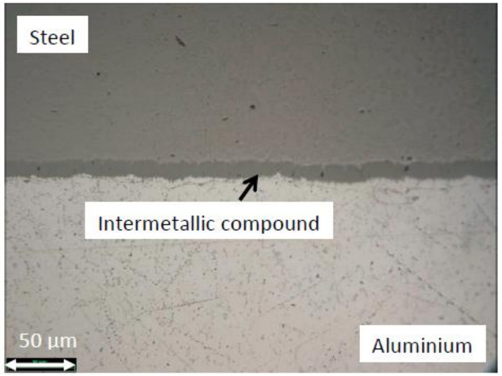

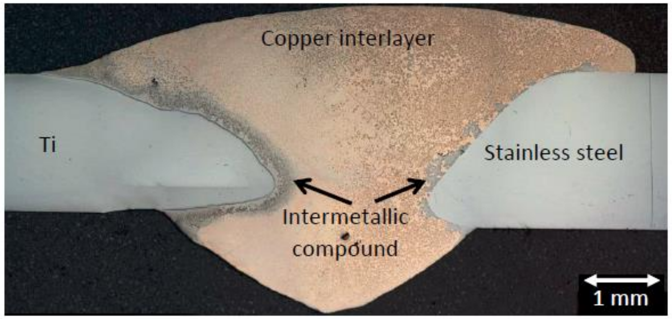

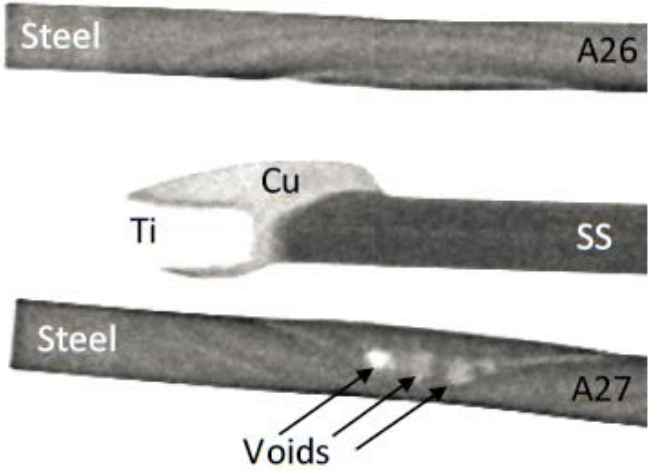

Full spectrum neutron radiography

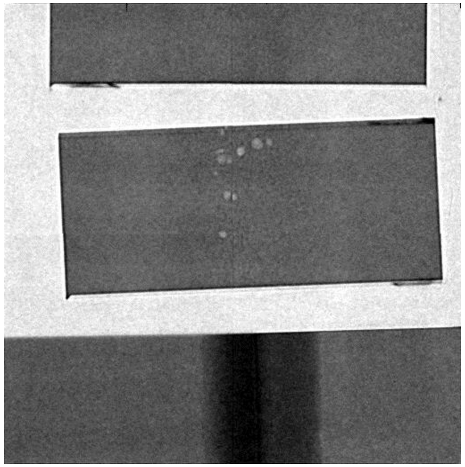

J. Appl. Crystallography **49** (2016) 1130

Dissimilar welds: SS to Titanium; Al to Steel

Narrow-energy images

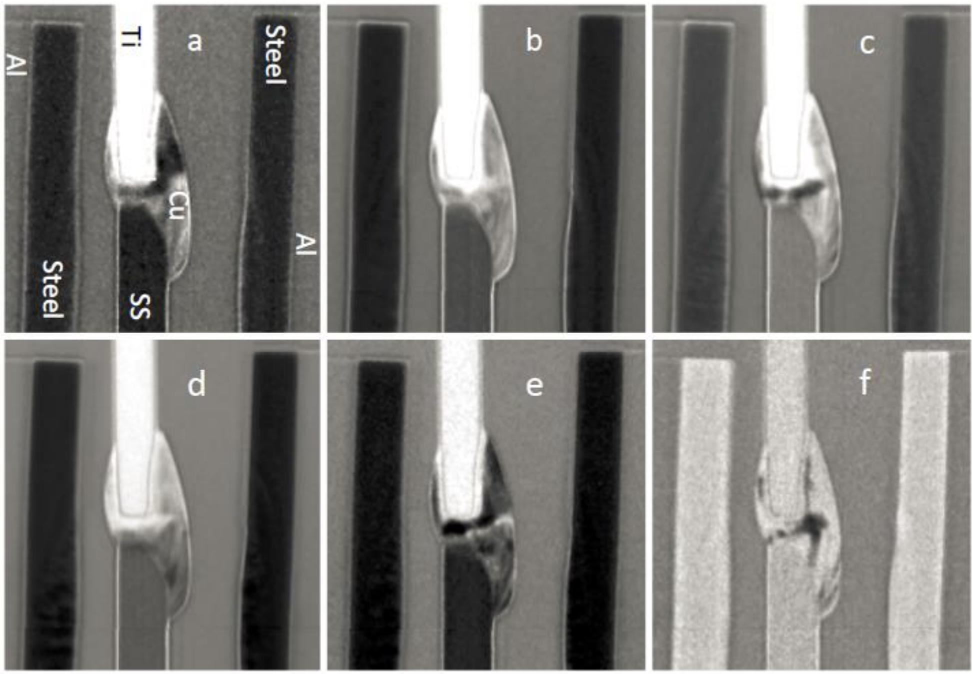

Texture within the Cu filler

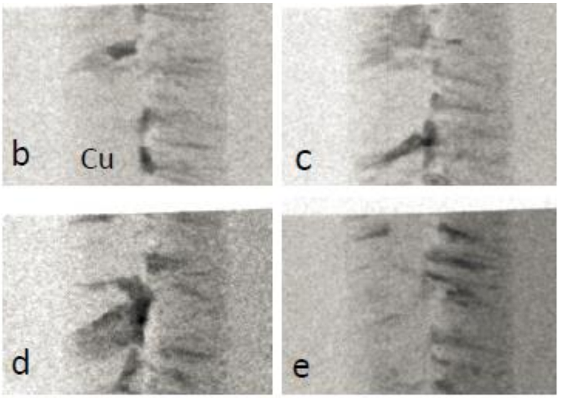

Heat affected zone is visible in steel

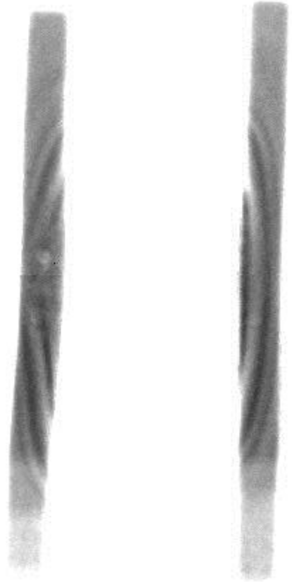

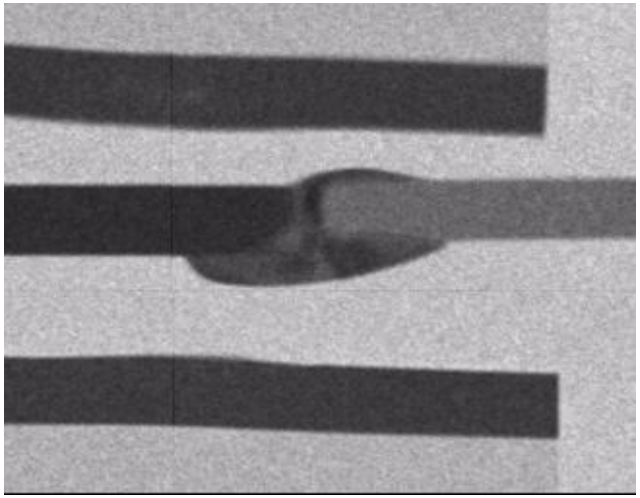

J. Appl. Crystallography **49** (2016) 1130

Bragg edge analysis

- T (~1 μs) relative to source trigger and position (~55 μm) for every neutron
- Transmission spectra within given area is calculated
- Limited statistics per 55x55 μm^2 pixel around Bragg edges - need to integrate data from several pixels

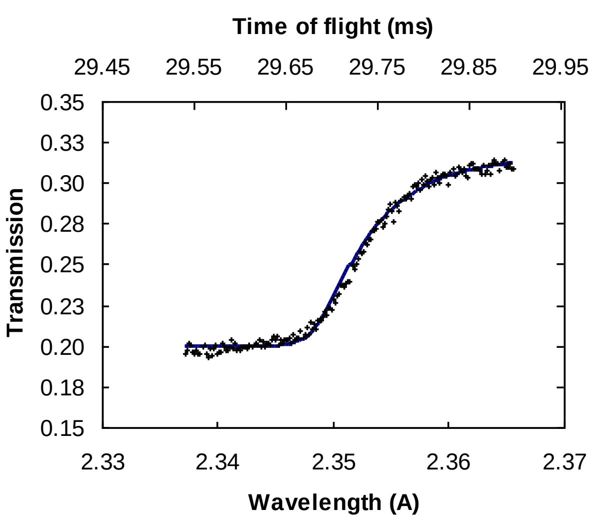

$$T(\lambda)\Big|_{\lambda_0,\sigma,\tau,C_1,C_2} = C_1 + C_2\left[erfc\left(\frac{\lambda_0-\lambda}{\sqrt{2}\sigma}\right) - \exp\left(\frac{\lambda_0-\lambda}{\tau}+\frac{\sigma^2}{2\tau^2}\right) * erfc\left(\frac{\lambda_0-\lambda}{\sqrt{2}\sigma}+\frac{\sigma}{\sqrt{2}\tau}\right)\right]$$

$$\frac{d(x,y)-d_0}{d_0} = \frac{\lambda(x,y)-\lambda_0}{\lambda_0}$$

Do the fit for every pixel – 262144 fits of coefficients

Very efficient and fast analysis tools are needed

Dissimilar welds: SS to Titanium; Al to Steel

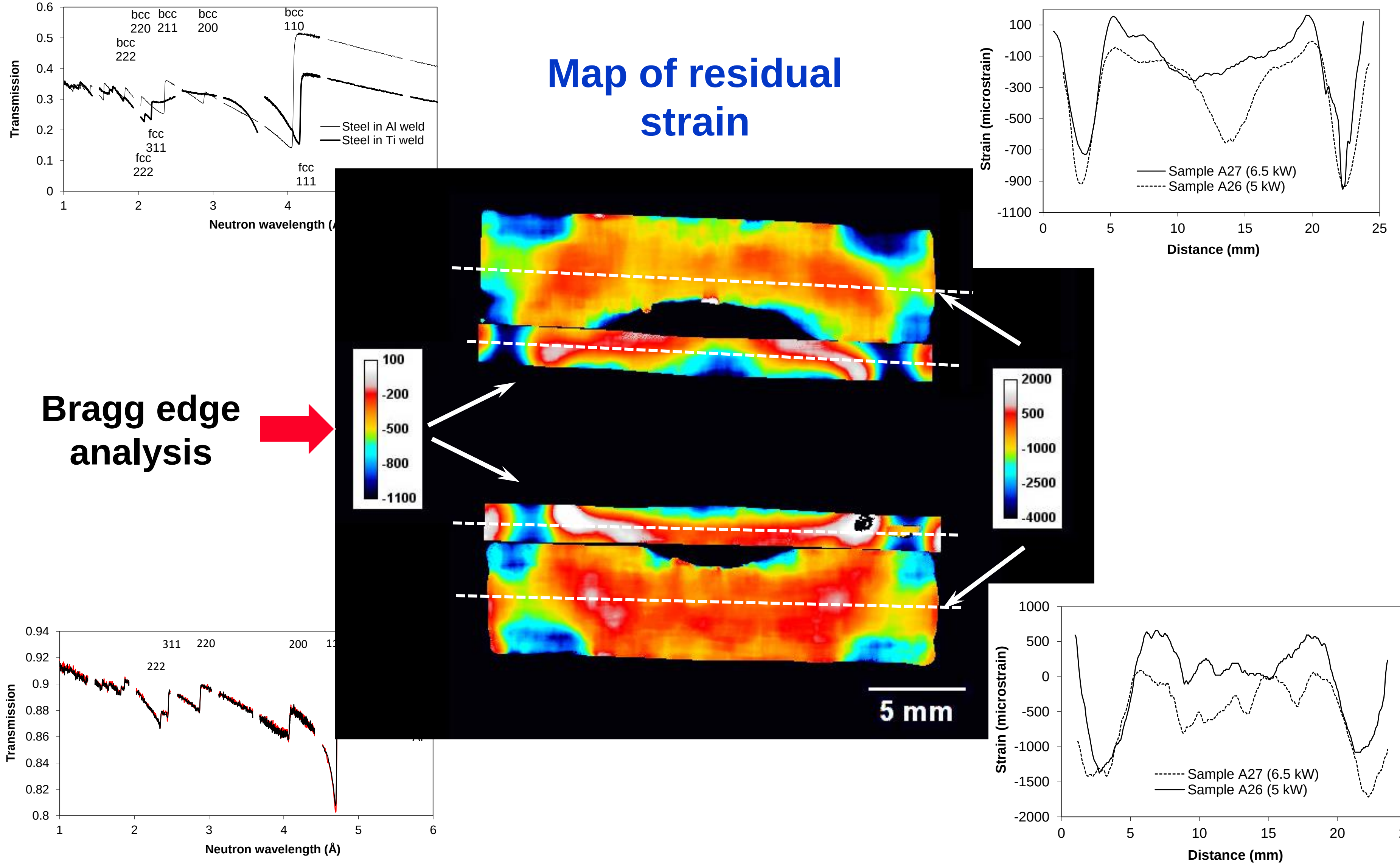

J. Appl. Crystallography **49** (2016) 1130-1140

Element-specific imaging through resonances

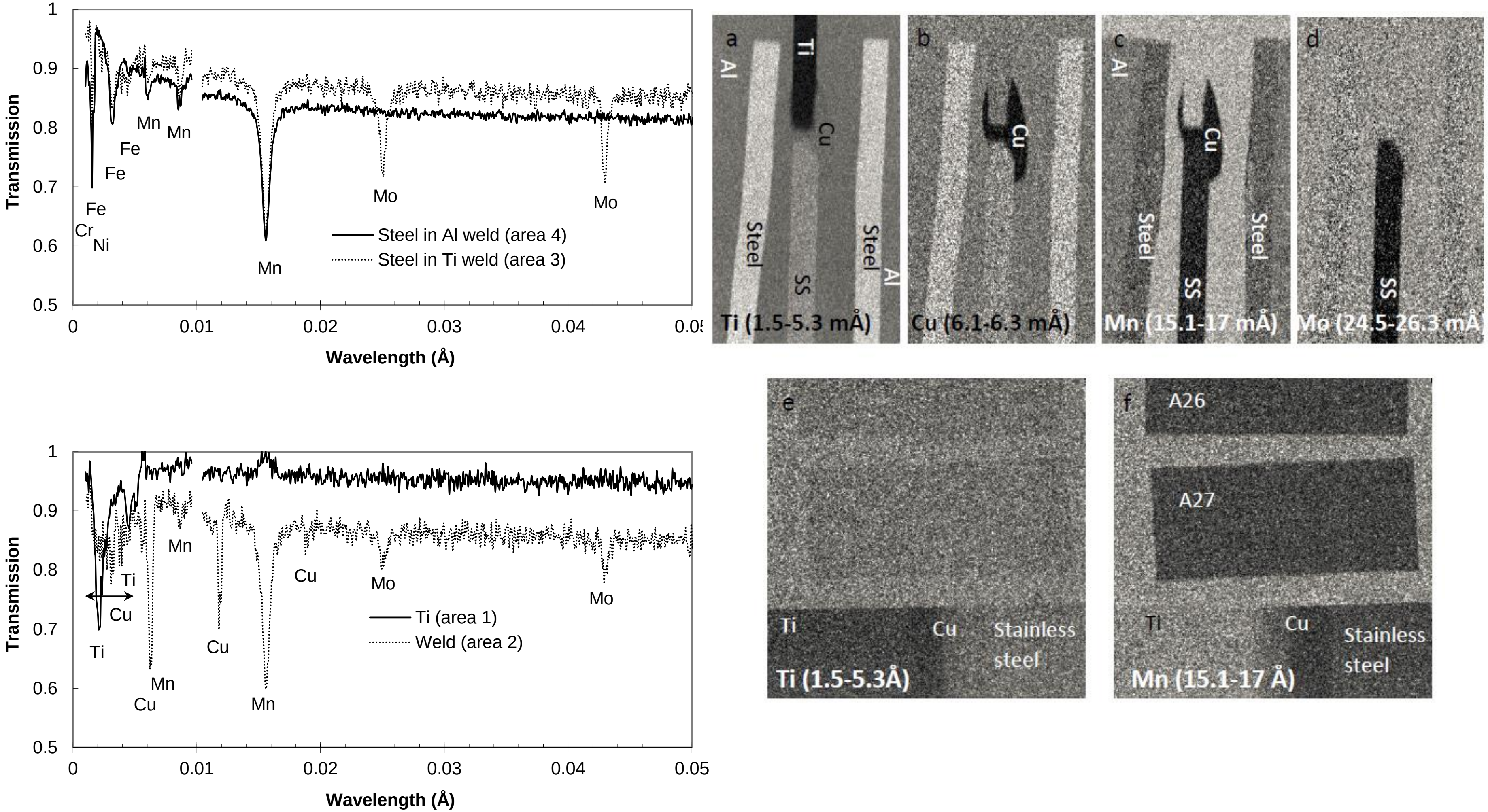

J. Appl. Crystallography **49** (2016) 1130-1140

Crystallographic properties through neutron scattering

Full spectrum radiography

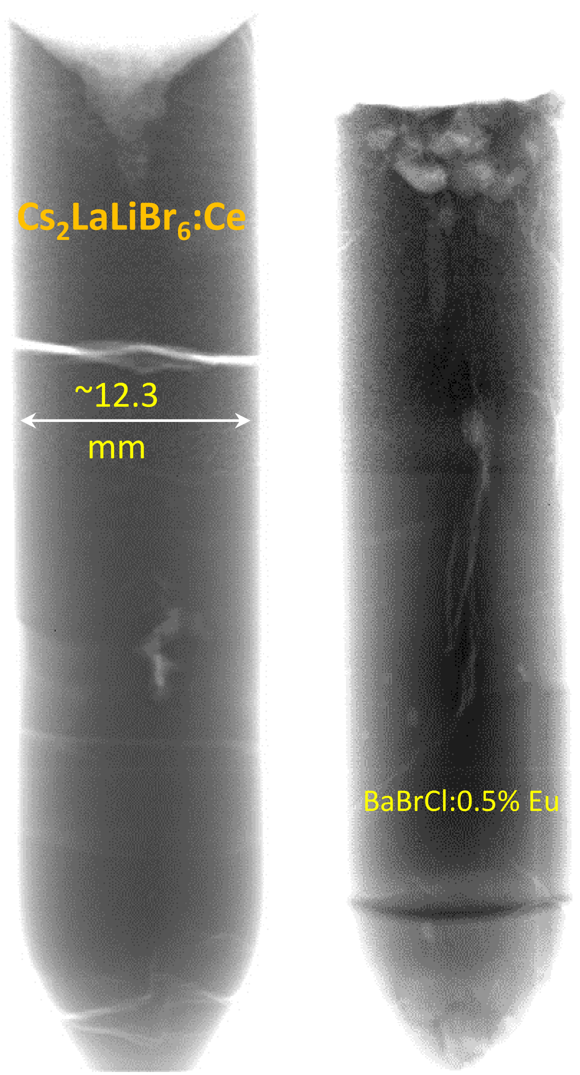

Scan through thermal energies:

Strong variation of crystal structure.
Not single crystal materials.

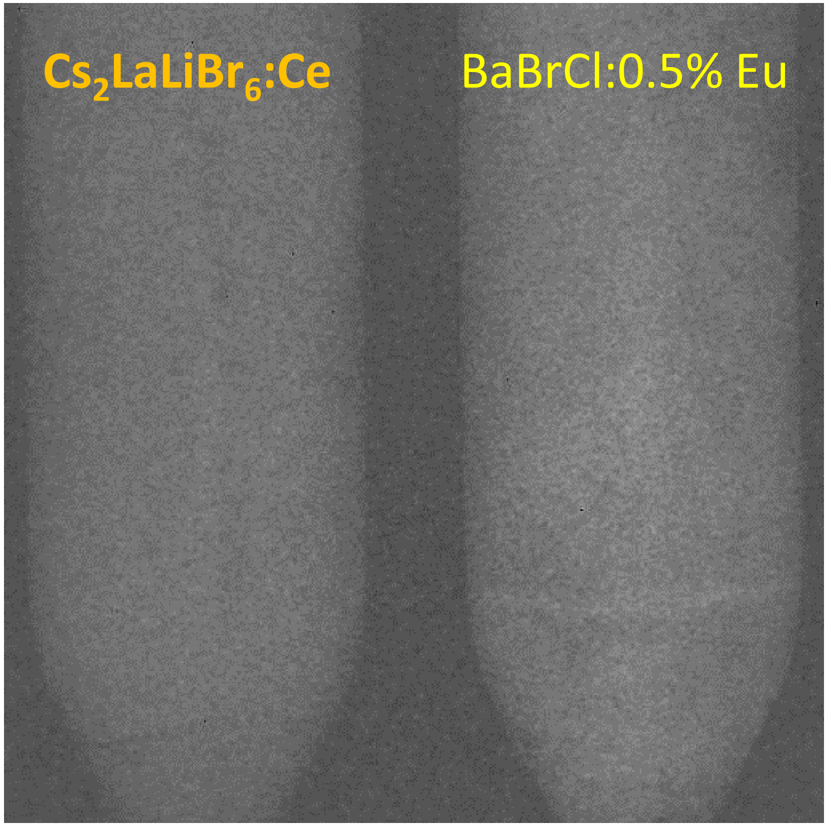

Liquid/solid interface: BaBrCl:5%Eu scintillator

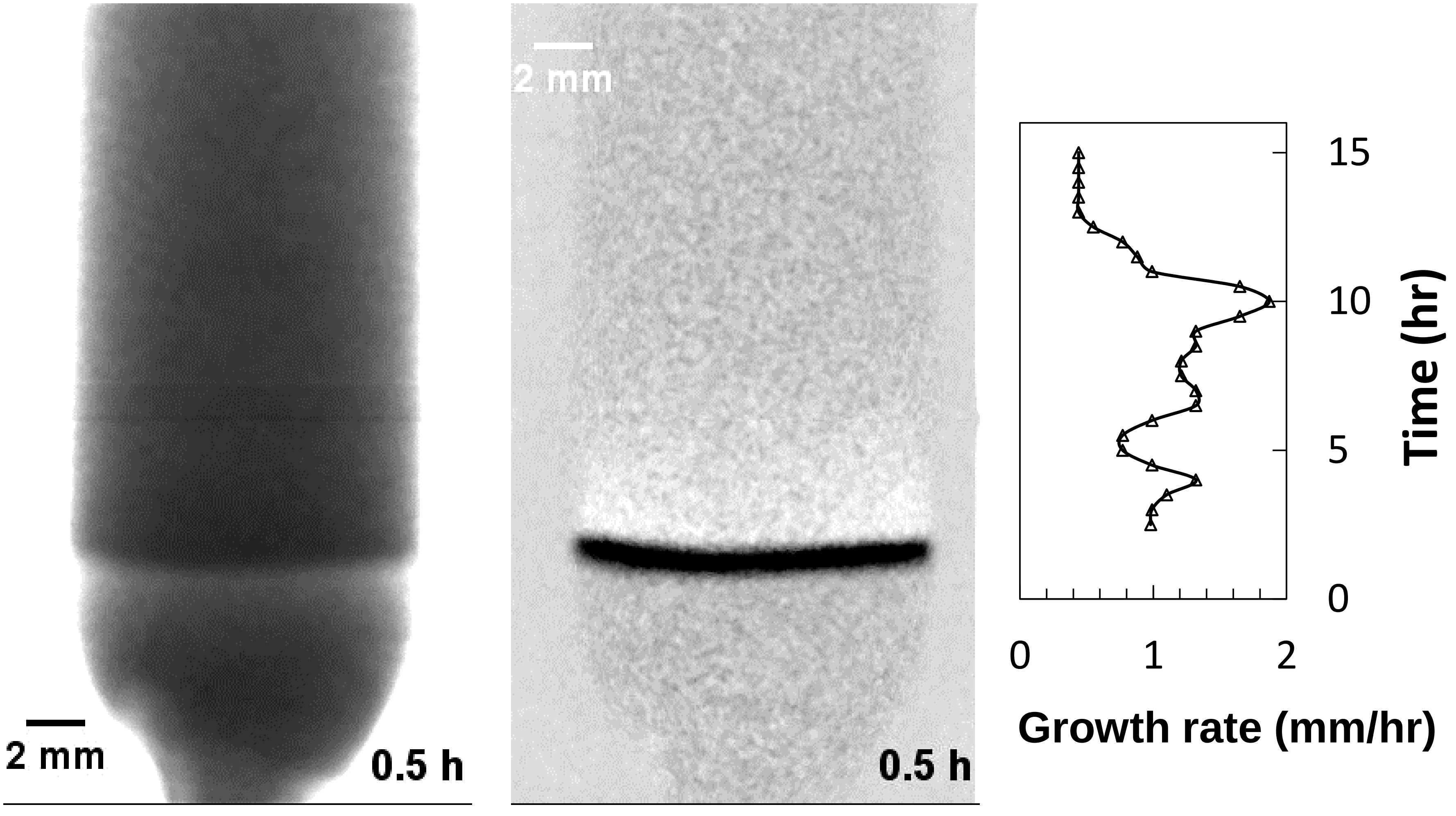

Scientific Reports 7 (2017) 46275

Eu concentration vs growth rate

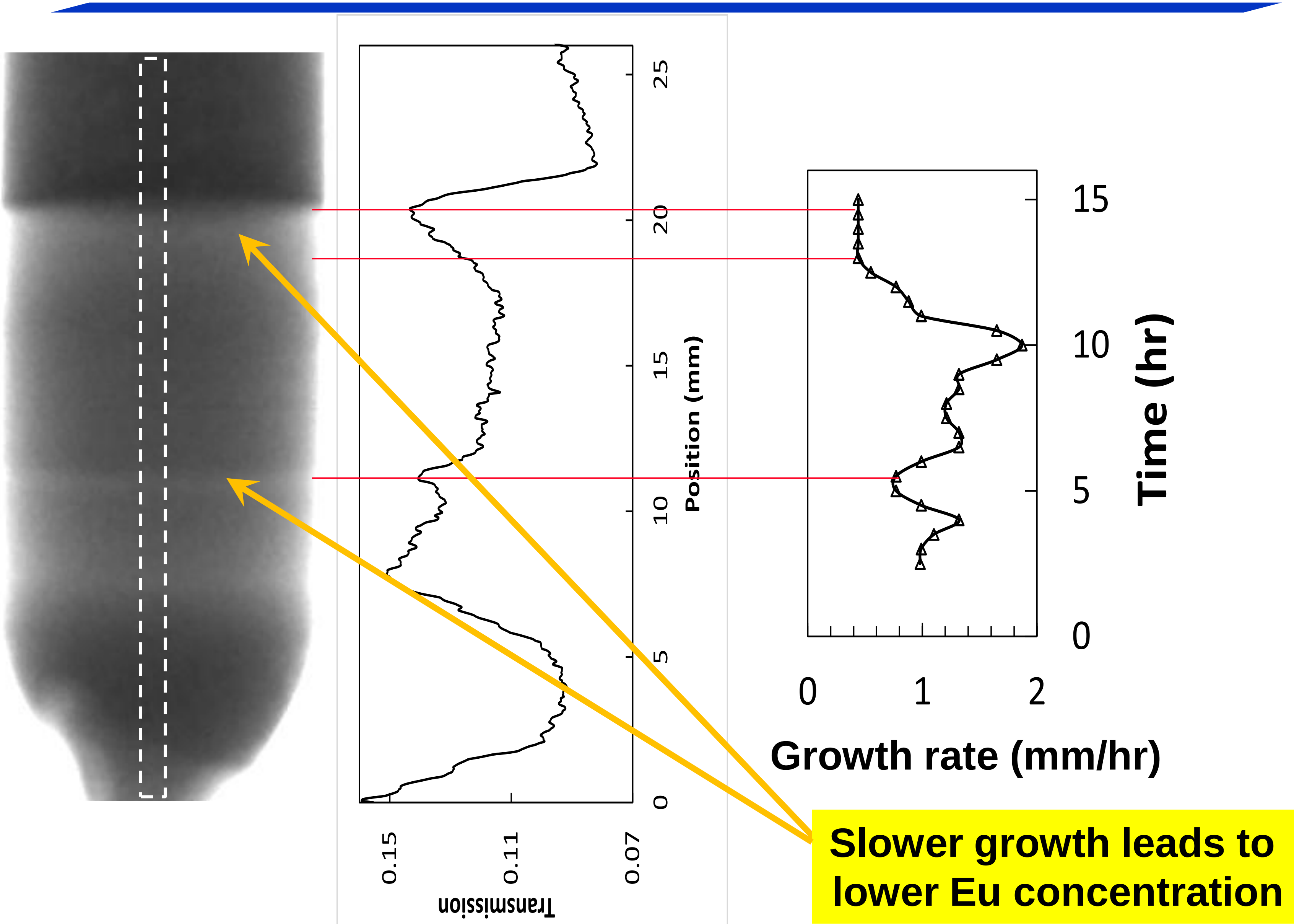

Liquid/solid interface: BaBrCl:Eu scintillator

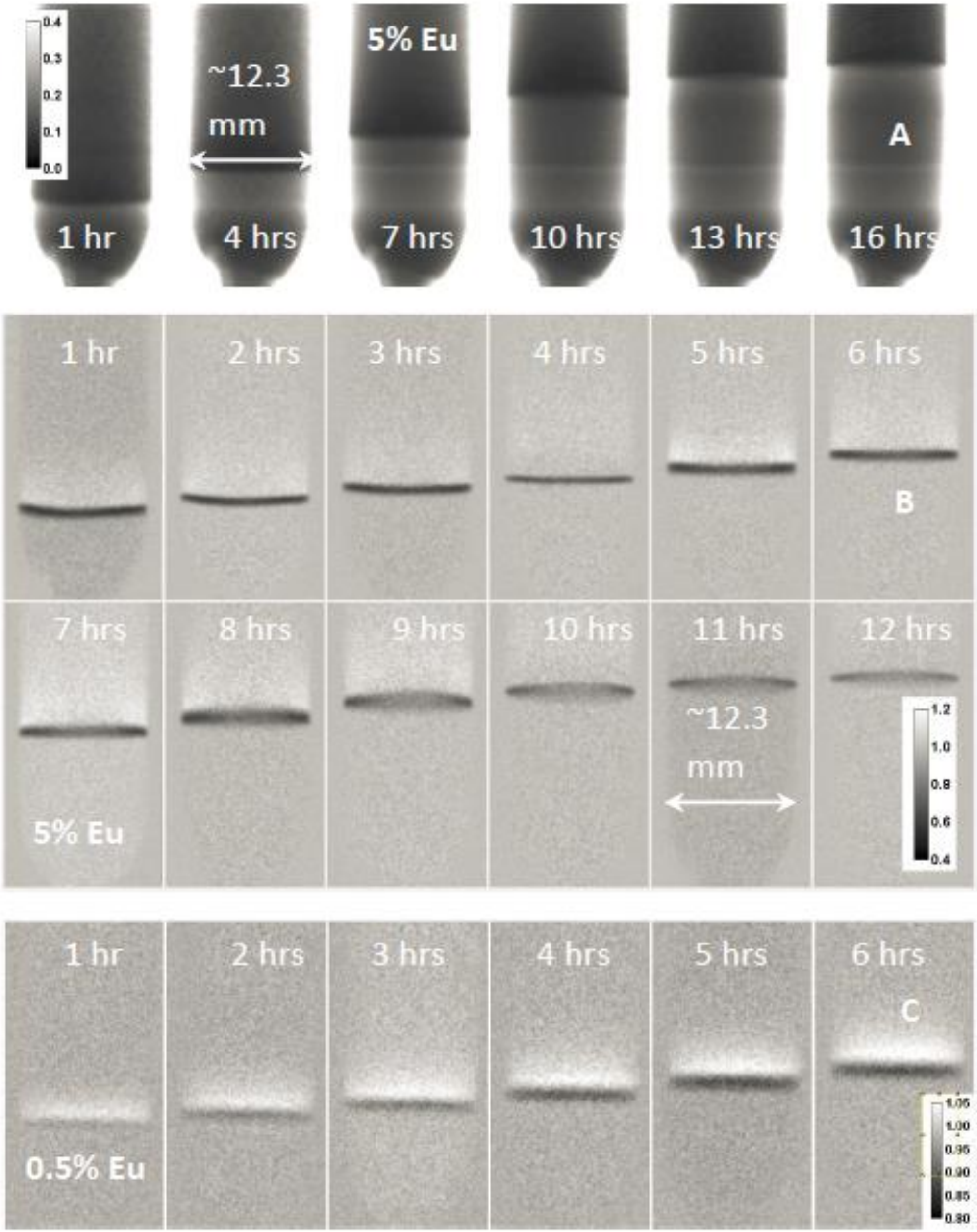

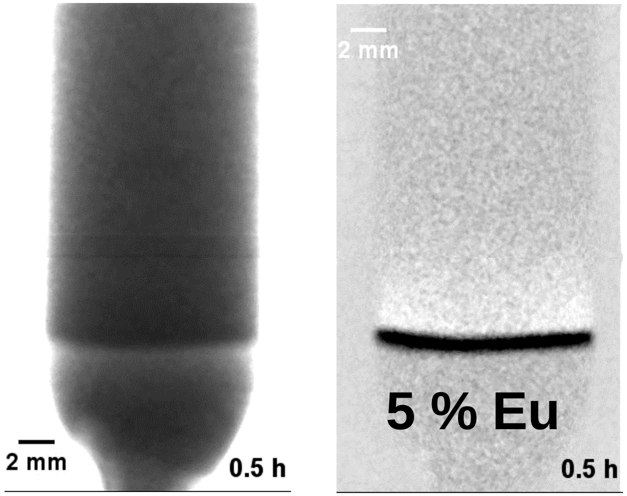

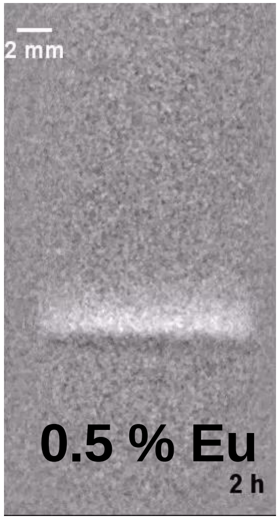

Element-specific imaging (5 % Eu sample)

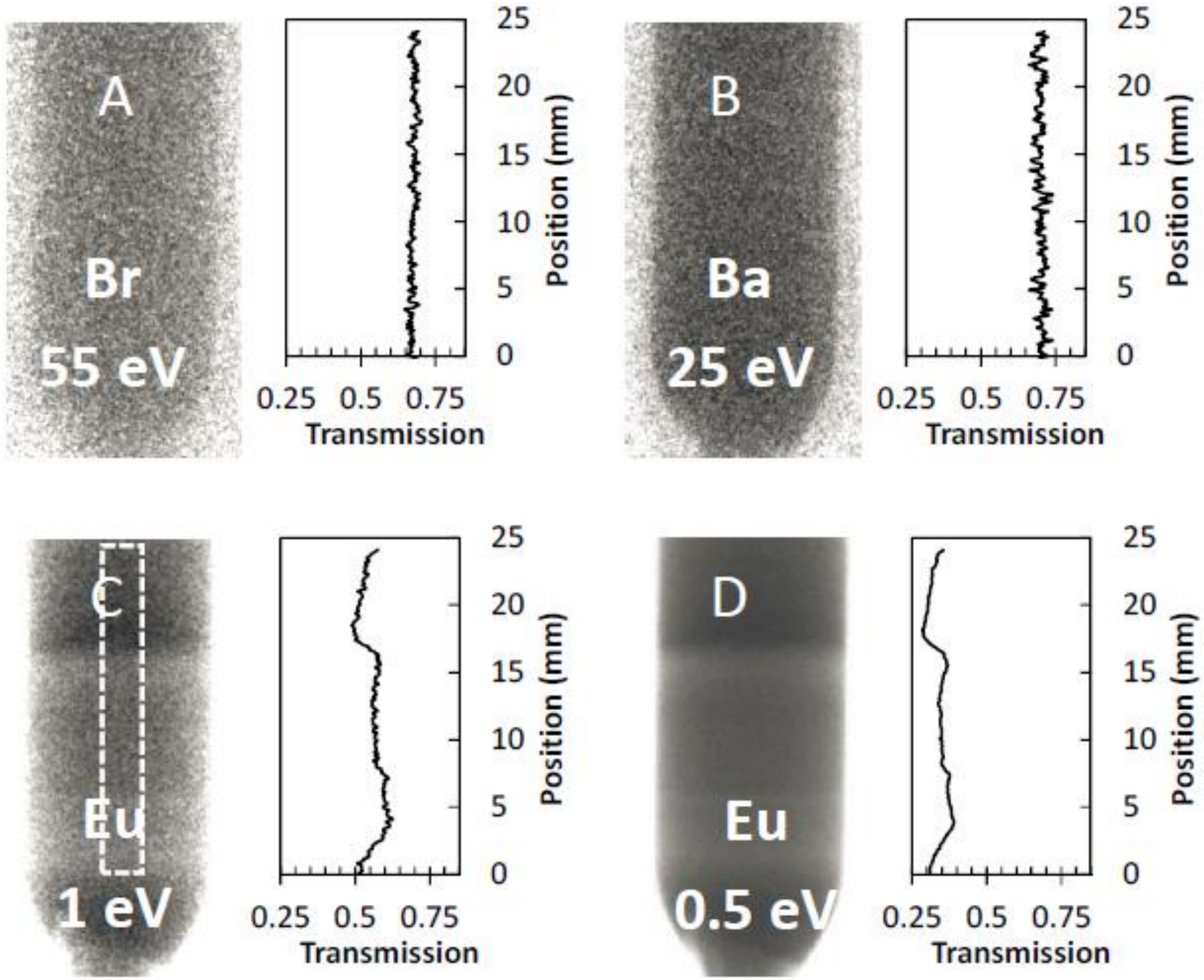

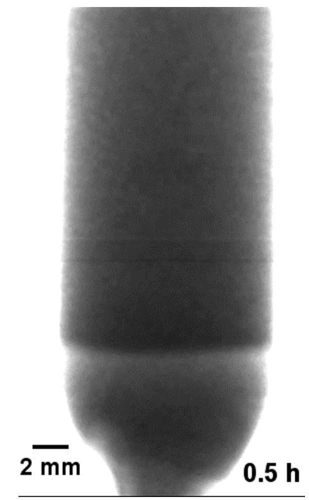

Scientific Reports 7 (2017) 46275

In situ Eu distribution quantification

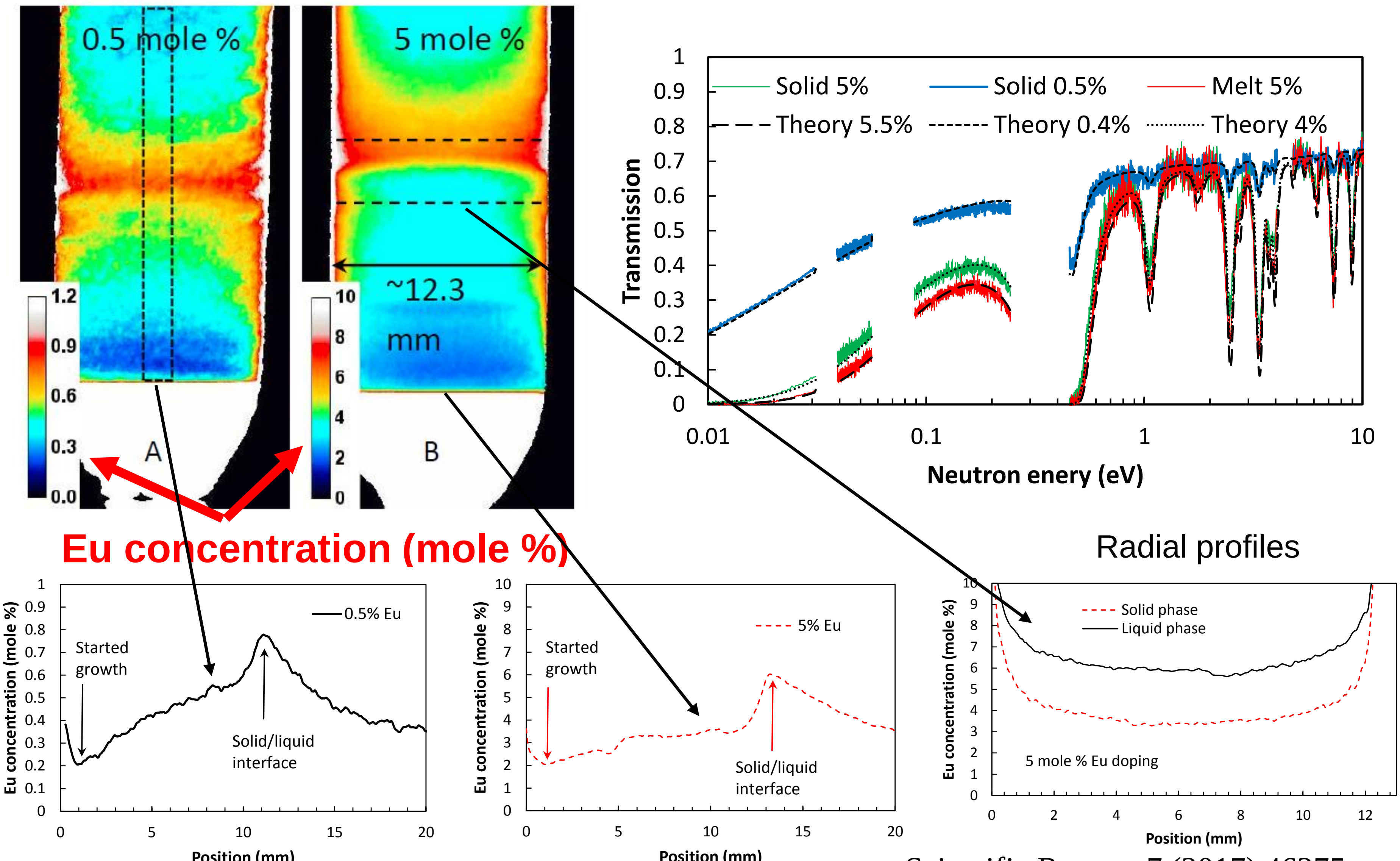

Vertical profiles

Scientific Reports 7 (2017) 46275